RESEARCH

2009-42

Asphalt Mixture and Binder Fracture Testing for 2008 MnROAD Construction

MnROAD
Office of Materials

Take the steps... Research...Knowledge...Innovative Solutions!

Transportation Research

Technical Report Documentation Page

1. Report No.	2.	3. Recipients Accession No.	
MN/RC 2009-42			
4. Title and Subtitle Asphalt Mixture and Binder Fracture Testing for 2008 MnROAD Construction		5. Report Date December 2009 6.	
7. Author(s) Mihai Marasteanu, Ki Hoon Moon, Mugurel Turos		8. Performing Organization Report No.	
9. Performing Organization Name and Address Department of Civil Engineering University of Minnesota 500 Pillsbury Drive SE Minneapolis, MN 55455		10. Project/Task/Work Unit No. 11. Contract (C) or Grant (G) No. (c) 89261 (wo) 105	
12. Sponsoring Organization Name and Address Minnesota Department of Transportation Research Services Section 395 John Ireland Boulevard, MS 330 St. Paul, MN 55155		13. Type of Report and Period Covered Final Report 14. Sponsoring Agency Code	
15. Supplementary Notes (including report URL, if available) http://www.lrrb.org/pdf/200942.pdf			
16. Abstract (Limit: 200 words) This report summarizes the results of an experimental effort to characterize the low-temperature behavior of asphalt mixtures and binders from the recently reconstructed cells at the MnROAD facility. In depth analysis of the data was not part of this study; this will be accomplished in several concurrent research projects.			
17. Document Analysis/Descriptors Asphalt, Binders, Asphalt mixtures, Fracture properties, Creep properties, Thermal stresses, Bend tests, Notch tests		18. Availability Statement No restrictions. Document available from: National Technical Information Services, Springfield, Virginia 22161	
19. Security Class (this report) Unclassified	20. Security Class (this page) Unclassified	21. No. of Pages 39	22. Price

Asphalt Mixture and Binder Fracture Testing for 2008 MnROAD Construction

Final Report

Prepared by:

Mihai Marasteanu
Ki Hoon Moon
Mugurel Turos

Department of Civil Engineering
University of Minnesota

December 2009

Published by:

Minnesota Department of Transportation
Research Services MS 330
395 John Ireland Boulevard
St. Paul, MN 55155

TABLE OF CONTENTS

LIST OF TABLES

LIST OF FIGURES

EXECUTIVE SUMMARY

Good fracture properties are an essential requirement for asphalt pavements built in the northern part of the US and in Canada for which the predominant failure mode is cracking due to high thermal stresses that develop at low temperatures. Currently, there is no agreement with respect to what experimental methods and analyses to use to investigate the fracture resistance of asphalt materials. This report summarizes the results of an experimental effort to characterize the low-temperature behavior of asphalt mixtures and binders from the recently reconstructed cells at the MnROAD facility. In depth analysis of the data was not part of this study; this will be accomplished in several concurrent research projects.

INTRODUCTION

A summary that details the laboratory sample preparation and test methods used in this research effort is provided in this report. The objective of this effort was to obtain laboratory test data on the low-temperature fracture properties of asphalt binders and mixtures used in the 2008 MnROAD reconstruction project. In depth analysis of the data was not part of this study; this will be accomplished in several concurrent research projects.

The University of Minnesota has already delivered the raw data files and Excel files with the results and partial analyses as part of the deliverables for each task. Testing was performed on the asphalt mixtures and binders samples described in Table 1 and Table 2, respectively.

Table 1. Asphalt mixtures tested.

ID	Cell	Mix type	Description	PG	RAP	Comments
A	2	Novachip		64-34	none	
B	2	SPWEB440F	level 4 Superpave	64-34	none	
C	*5*	*PASSRC*	*permeable stress relief course*	*64-22*	*none*	*Couldn't be compacted Replaced by M*
D	6	SPWEB440 F Special	4.75 taconite Superpave	64-34	none	
E	16	SPWEB440 C Special	warm asphalt wear course	58-34	20%	
F	16	SPWEB430 C Special	warm asphalt nonwear	58-34	20%	
G	20	SPNWB430 B	non wear	58-28	30% non fractionated	
H	21	SPNWB430 B Special	non wear	58-28	30% fractionated	
I	22	SPNWB430 C Special 1	non wear	58-34	30% fractionated	
J	86,88	SPWEB440 H Special 1	porous asphalt	70-28	none	
	87	*SPWEB340B*	*level 3 Superpave*	*58-28*	*20%*	*Not available Replaced by K*
K	5	SPWEB440B	shoulder mix	58-28	5% manufactured waste shingles	
L	24	SPWEB440C	control for warm mix asphalt	58-34	20 %	
M	15,17 21	SPWEB440B	shoulder mix	58-28	5% tear off shingles	

Table 2. Asphalt binders tested.

ID
PG 70-28
PG 64-34
PG 64-22
PG 58-34 (WMA)
PG 58-34
PG 58-28
extracted RAP (standard)
extracted RAP (coarse)
extracted RAP (fine)

For each mixture the theoretical maximum specific gravity G_{mm} and the bulk specific gravity G_{mb} (at N_{des}) were determined according to AASHTO T 209-05 and AASHTO T 166-05. The air voids were calculated as $1 - (G_{mb} / G_{mm})$ and expressed in percentage. The values are presented in the Table 3.

Table 3. Specific gravities for the asphalt mixtures.

Loose mix type	G_{mb}	G_{mm}	Air Voids
A	2.362	2.493	5.3%
B	2.412	2.499	3.5%
D	2.436	2.563	5.0%
E	2.397	2.517	4.8%
F	2.437	2.499	2.5%
G	2.435	2.518	3.3%
H	2.432	2.528	3.8%
I	2.416	2.514	3.9%
J	2.06	2.558	19.5%
K	2.418	2.534	4.6%
L	2.392	2.524	5.2%
M	2.378	2.608	8.8%

Using the compaction data, a target weight and height were calculated for each mixture to achieve the desired value of 7% air voids. Two exceptions were observed. It was difficult to obtain the G_{mb} value for the porous mix "J"; due to the high air voids content, a lot of water

drained out when the cylinder was moved from the bath to the scale. In this case the target was set to 100 gyrations for the test cylinders. Mixture "M", after 100 gyrations, still had 8% air voids. For the test specimens the target was set to 100 gyrations.

For each mixture eight cylinders were compacted. If needed, after the first two cylinders the target was adjusted to obtain a better match. Out of them, four were tested in the laboratory, and two were sent back to the Minnesota Department of Transportation (Mn/DOT). The target values and the air voids are shown in Table 1.4.

Table 4. Air voids for the compacted loose mix cylinders.

Mix ID	Target		Cylinder ID									
	Weight, g	Height, mm	1	2	3	4	5	6	7	8	UofM	Mn/DOT
A	6900	172.97	7.9	7.1	7	7.1	7.2	7.2	6.8	7	2.3.4.5	6&8
B	7125	174.72	7.5	7.6	7.4	7.8	6.6	6.5	6.9	6.4	1,2,3,5	6&7
D	7325	174.72	7.3	7.6	7.6	7.5	6.5	7	6.8	6.7	1.2.4.6	7&8
E	7200	175.83	7.2	7.2	7	7.1	7	7	6.9	7	3.4.5.6	7&8
F	7100	175.50	7.3	7.5	7.1	7.4	7.2	7.1	7.7	7.1	1.3.4.5	6&8
G	7200	175.83	6.95	6.95	6.85	6.9	6.9	6.8	6.7	6.8	1.2.3.4	5&8
H	7200	175.20	6.7	7.1	7.1	7.1	6.8	6.8	6.7	7	2.3.4.5	6&8
I	7200	175.86	7	7	6.6	7.1	7.1	6.9	7	7	1.2.4.5	7&8
J	6100	*100 gyr*	19.7							19	3.4.5.6	7&8
K	7200	174.50	7.2	7.3	7	7.5	7.4	7.3	7.5	7.2	1.2.3.6	7&8
L	7100	173.00	7.5	7.5	7.2	7.2	7	7	7.2	7.3	3.4.5.6	7&8
M	7300	*100 gyr*	8.8	8.8	8	8	8	8.1	8	8.1	3.4.5.6	7&8

For the performance tests, the compacted cylinders were not subject to any long-term aging in the laboratory. The mixtures were only heated long enough to split into the proper weights and then heated to the compaction temperature (or something like that – describe the process).

TASK 1

This task consisted of sample preparation and Semi Circular Bend (SCB) testing on the mixtures described in Table 1. The SCB tests were conducted on each mix at three test temperatures (at a single air void and laboratory conditioning level) with three replicates per temperature. The test temperatures were selected based on the PG of the binder as follows:

- PG +10°C
- 12°C below (PG +10°C)
- 12°C above (PG +10°C).

A MTS servo-hydraulic testing system equipped with an environmental chamber was used to perform the SCB test. The SCB samples were symmetrically supported by two fixed rollers and had a span of 120mm. Teflon tape was used to reduce the friction from the two rollers. The Indirect Tension test (IDT) loading plate was used to load the SCB specimens. The load line displacement (LLD) was measured using a vertically mounted Epsilon extensometer with 38 mm gage length and ±1 mm range; one end was mounted on a button that was permanently fixed on a specially made frame, and the other end was attached to a metal button glued to the sample. The crack mouth opening displacement (CMOD) was recorded by an Epsilon clip gage with 10 mm gage length and a +2.5 and -1 mm range. The clip gage was attached at the bottom of the specimen. Considering the brittle behavior of asphalt mixtures at low temperatures, the CMOD signal was used as the control signal to maintain the test stability in the post-peak region of the test. A constant CMOD rate of 0.0005mm/s was used and the load and load line displacement (P-u) curve was plotted. A contact load with maximum load of 0.3 kN was applied before the actual loading to ensure uniform contact between the loading plate and the specimen. The testing was stopped when the load dropped to 0.5 kN in the post peak region. All tests were performed inside an environmental chamber. Liquid nitrogen was used to obtain the required low temperature. The temperature was controlled by the environmental chamber temperature controller and verified using an independent thermometer.

The load and load line displacement data were used to calculate the fracture toughness and fracture energy. It was shown that the stress intensity factor K can be reasonably calculated using the following equation:

$$\frac{K_I}{\sigma_0\sqrt{\pi a}} = Y_I(s_0/r) + \frac{\Delta s_0}{r}B \qquad [1]$$

where

K_I = Mode I stress intensity factor;

σ_0 = $P/2rt$

P = applied load;

r = specimen radius;

t = specimen thickness.

Y_I = the normalized stress intensity factor

$$Y_{I(s_0/r)} = C_1 + C_2(a/r) + C_3\exp(C_4(a/r)) \qquad [2]$$

C_i = constants;

a = notch length;

$\Delta s_0/r = s_a/r - s_0/r$

s_a/r = actual span ratio;

s_0 / r = nearest span ratio analyzed in the derivation of this equation (0.80, 0.67, 0.61, 0.50)

$$B = 6.55676 + 16.64035(\frac{a}{r})^{2.5} + 27.97042(\frac{a}{r})^{6.5} + 215.0839(\frac{a}{r})^{16}$$

The fracture energy G_f was calculated according to RILEM TC 50-FMC specification that has been extensively used in the study of concrete. The work of fracture is the area under the loading-deflection (P-u) curve and the fracture energy (G_f) can then be obtained by dividing the work of fracture with the ligament area, which is calculated as the product of the ligament length and the thickness of the specimen. This is shown in equation 3.

$$G_f = \frac{W_f}{A_{lig}} \qquad [3]$$

where W_f is the work of fracture and

$$W_f = \int P du$$

A_{lig} is the area of the ligament.

The tail part of the P-u curve can be reasonably obtained by fitting the data curve in the post-peak region following two methods described elsewhere (Li 2005, Marasteanu et al, 2007). In the first method, the area of the tail was computed as

$$W_{tail} = \int_0^{peak\Delta L} \frac{a}{x^2} dx$$

In the second method, the area of the tail was computed as

$$W_{tail} = \int_0^{peak\Delta L} b \cdot x^c dx$$

Summary plots of the parameters obtained as a result of the tests in this task are shown in Figures 1 to 6 and in Tables 5 and 6.

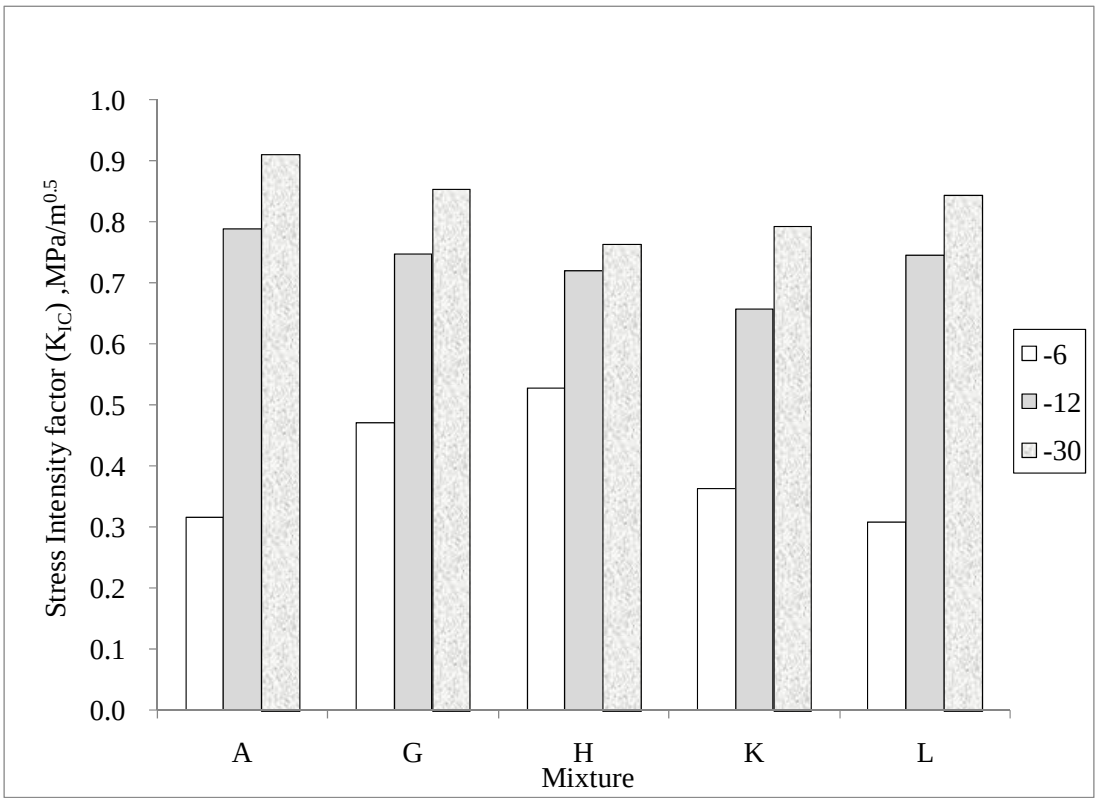

Figure 1. Mixture SCB fracture toughness values (mixtures A, G, H, K, L)

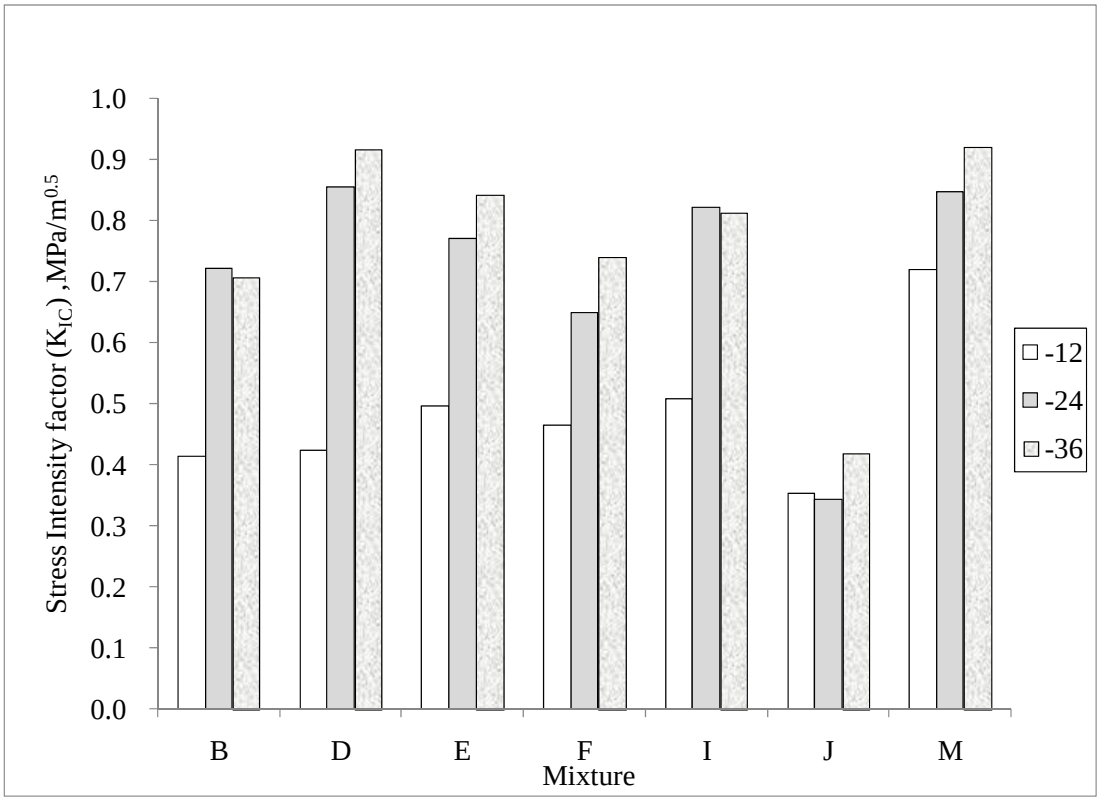

Figure 2. Mixture SCB fracture toughness values (mixtures B, D, E, F, I, J, M)

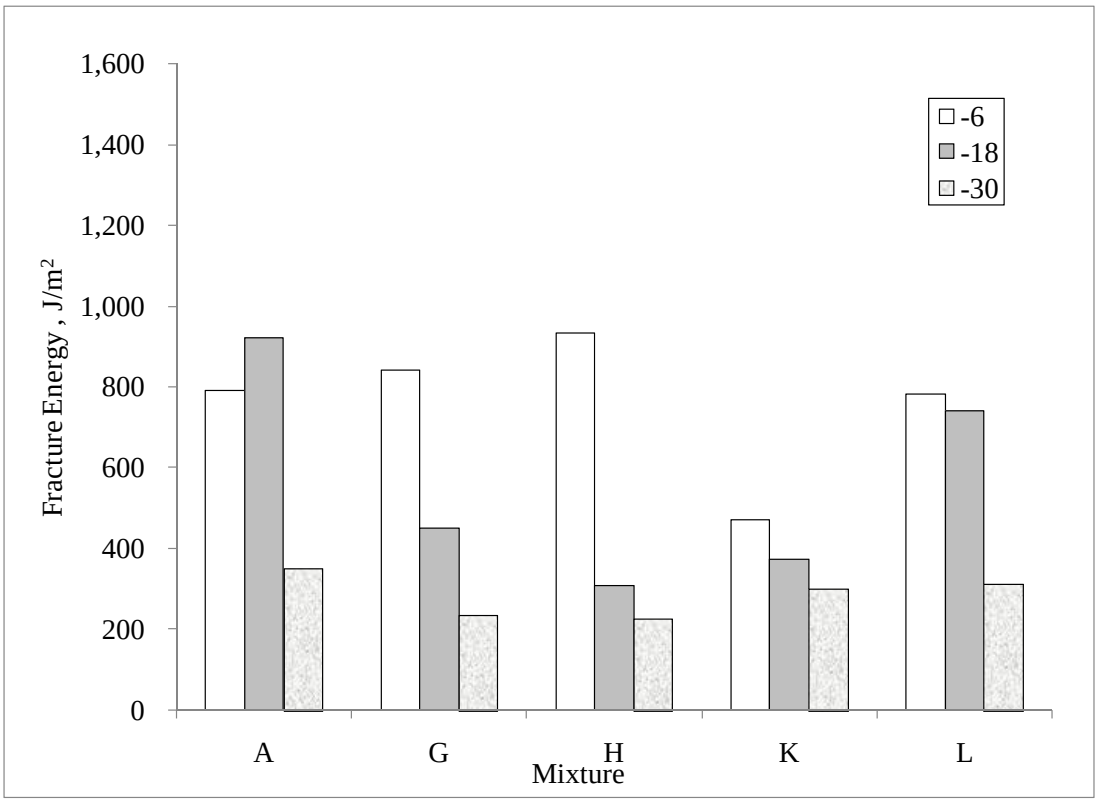

Figure 3. SCB fracture energy values obtained with method 1 (mixtures A, G, H, K, L)

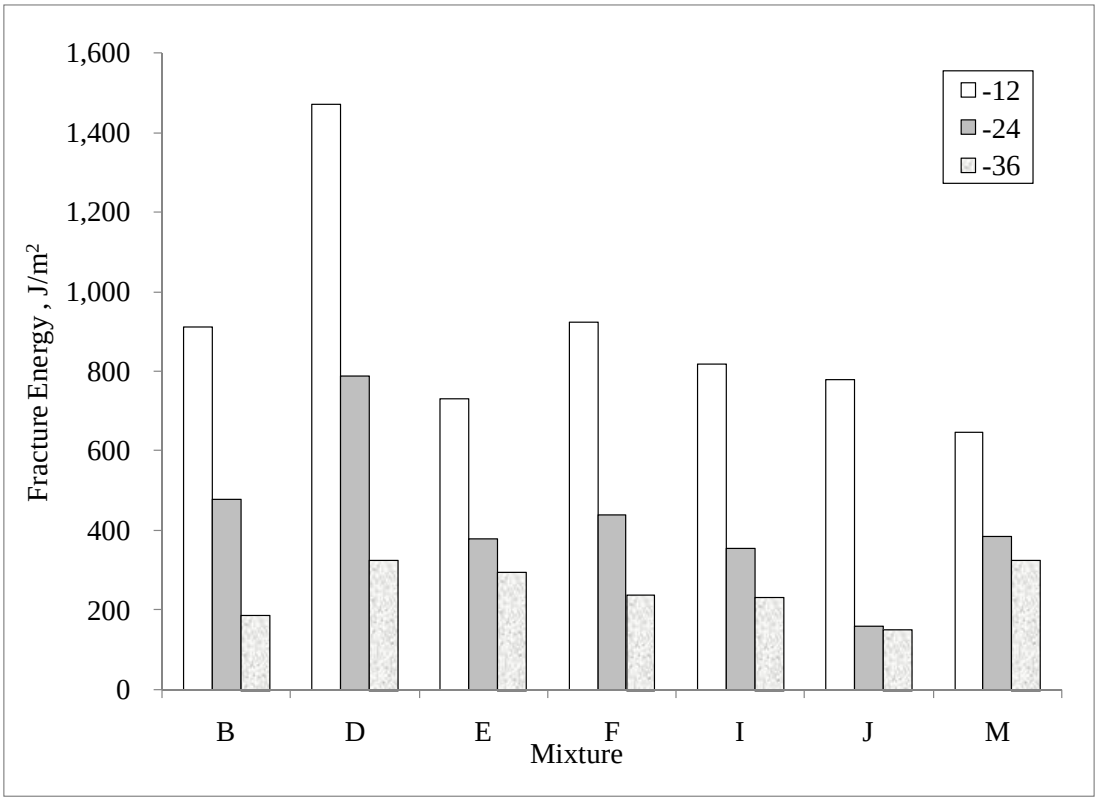

Figure 4. SCB fracture energy values obtained with method 1 (mixtures B, D, E, F, I, J, M)

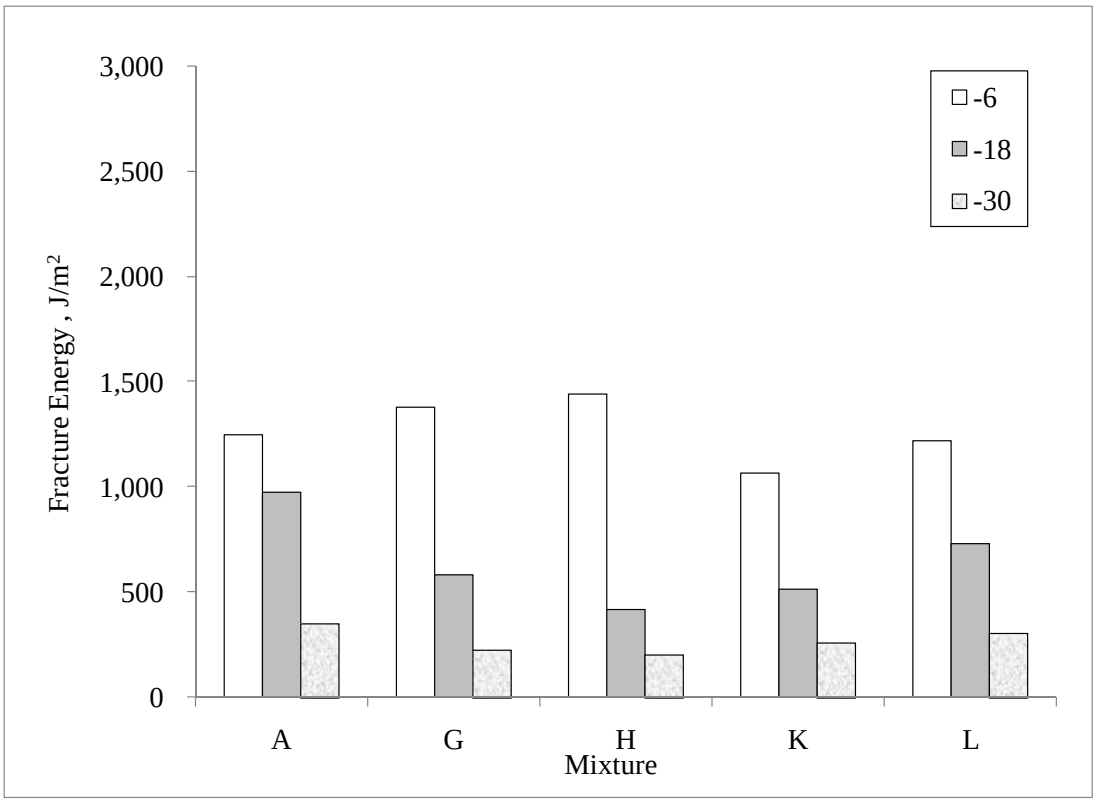

Figure 5. SCB fracture energy values obtained with method 2 (mixtures A, G, H, K, L)

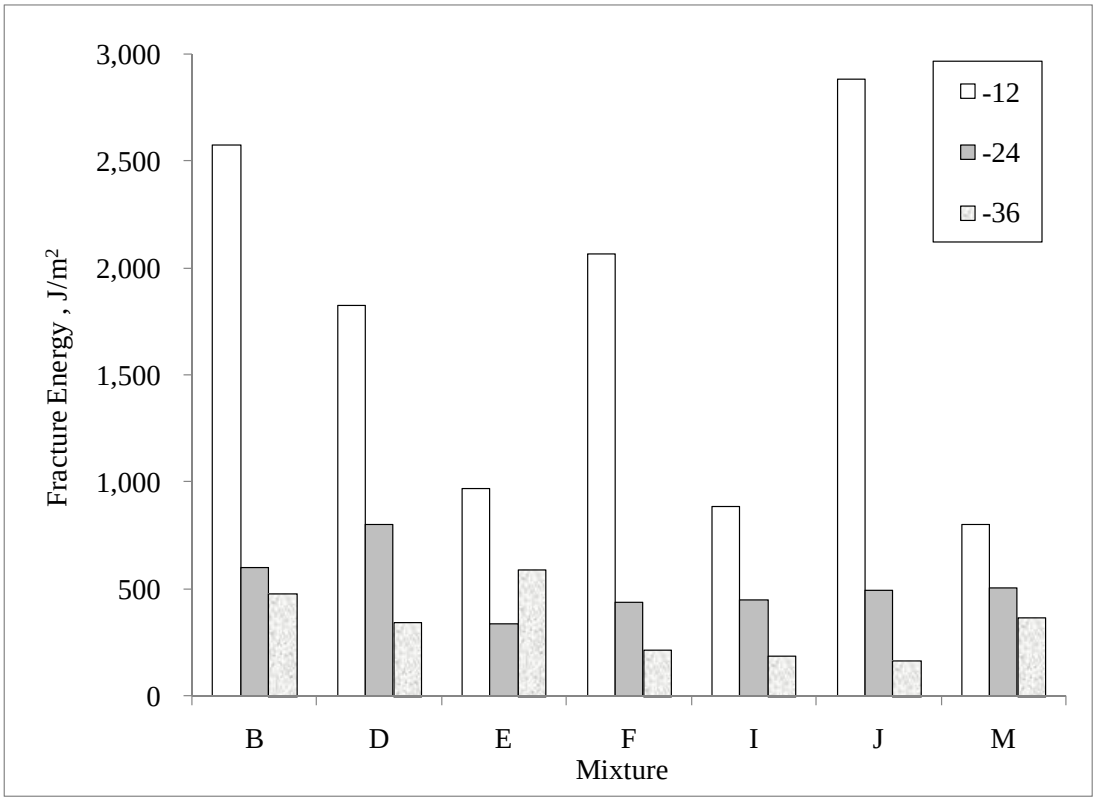

Figure 6. SCB fracture energy values obtained with method 2 (mixtures B, D, E, F, I, J, M)

Table 5. Summary of mixture SCB fracture toughness results.

Mix ID	T °C	K_{IC} (Stress intensity factor) , kPa/$m^{0.5}$				
		R1	R2	R3	Average	CV(%)
A	-6	302.8	374.4	268.1	315.1	17.2%
	-18	779.8	785.9	799.5	788.4	1.3%
	-30	886.6	909.3	935.5	910.5	2.7%
B	-12	348.8	482.2	412.1	414.3	16.1%
	-24	644.2	779.1	739.0	720.8	9.6%
	-36	679.3	793.5	649.5	707.4	10.8%
D	-12	440.4	415.1	417.6	424.4	3.3%
	-24	794.7	833.2	935.8	854.6	8.5%
	-36	917.0	918.4	OL	917.7	0.1%
E	-12	468.5	529.6	489.7	495.9	6.3%
	-24	812.7	797.9	703.7	771.4	7.7%
	-36	791.7	896.0	841.3	843.0	6.2%
F	-12	460.1	470.0	461.2	463.8	1.2%
	-24	635.3	683.4	630.0	649.6	4.5%
	-36	725.3	772.7	724.0	740.7	3.7%
G	-6	448.3	533.0	428.5	469.9	11.8%
	-18	697.2	716.6	824.5	746.1	9.2%
	-30	833.5	988.2	742.8	854.8	14.5%
H	-6	458.9	619.1	506.1	528.0	15.6%
	-18	716.3	608.4	832.0	718.9	15.6%
	-30	727.6	881.4	683.3	764.1	13.6%
I	-12	469.0	452.4	601.3	507.6	16.1%
	-24	794.6	826.5	845.7	822.2	3.1%
	-36	803.7	860.3	778.4	814.1	5.2%
J	-12	355.0	350.3	NA	352.7	0.9%
	-24	379.1	292.5	356.1	342.6	13.1%
	-36	389.1	449.0	422.0	420.0	7.1%
K	-6	344.0	307.8	433.8	361.8	17.9%
	-18	642.1	641.0	688.1	657.1	4.1%
	-30	763.5	762.8	856.6	794.3	6.8%
L	-6	292.0	336.5	293.5	307.4	8.2%
	-18	772.2	786.0	677.0	745.0	8.0%
	-30	710.9	819.0	1006.1	845.3	17.7%
M	-12	670.9	788.4	702.2	720.5	8.4%
	-24	873.5	770.5	898.7	847.6	8.0%
	-36	1019.0	835.4	910.3	921.6	10.0%

OL = Outlier

NA = Not Available

Table 6. Summary of mixture SCB fracture energy results.

Mix ID	T °C	G_f (fracture energy) , J/m^2, Method 1					G_f (fracture energy) , J/m^2, Method 2					D(%)
		R1	R2	R3	Ave	CV(%)	R1	R2	R3	Ave	CV(%)	
A	-6	749	1090	532	791	35.6%	1013	1997	723	1245	53.6%	36.5%
	-18	1035	821	911	922	11.7%	944	956	1020	973	4.2%	5.2%
	-30	343	401	310	351	13.1%	350	422	290	354	18.6%	0.8%
B	-12	868	1062	804	911	14.7%	3587	1308	2825	2573	45.1%	64.6%
	-24	303	579	551	478	31.8%	406	737	648	597	28.7%	20.0%
	-36	136	245	188	190	28.8%	OL	217	741	479	77.5%	60.4%
D	-12	1568	1404	1436	1469	5.9%	1787	1648	2042	1826	10.9%	19.5%
	-24	646	883	839	789	15.9%	746	861	788	798	7.3%	1.1%
	-36	347	305	OL	326	8.9%	282	416	OL	349	27.3%	6.6%
E	-12	774	731	690	731	5.7%	1392	694	822	969	38.4%	24.5%
	-24	441	335	362	380	14.5%	398	312	290	334	17.1%	13.8%
	-36	356	237	296	296	20.0%	898	367	511	592	46.4%	49.9%
F	-12	910	900	956	922	3.2%	2942	1505	1744	2064	37.3%	55.3%
	-24	276	373	666	438	46.4%	446	431	OL	438	2.3%	0.0%
	-36	277	224	217	239	13.7%	246	200	211	219	11.1%	9.3%
G	-6	950	811	766	843	11.4%	1029	1071	2024	1375	40.9%	38.7%
	-18	394	387	566	449	22.6%	410	660	669	580	25.3%	22.5%
	-30	207	293	207	236	21.1%	173	296	210	226	27.9%	4.3%
H	-6	1027	984	787	933	13.7%	1734	OL	1150	1442	28.6%	35.3%
	-18	340	213	375	310	27.6%	361	OL	472	416	18.9%	25.6%
	-30	212	208	257	226	12.1%	197	OL	219	208	7.5%	8.7%
I	-12	725	831	895	817	10.5%	OL	952	813	882	11.1%	7.4%
	-24	352	371	341	355	4.3%	OL	535	360	448	27.5%	20.8%
	-36	274	222	205	234	15.4%	OL	191	184	188	2.6%	24.3%
J	-12	787	770	NA	778	1.6%	1830	3938	NA	2884	51.7%	73.0%
	-24	146	105	226	159	38.7%	178	526	771	492	60.6%	67.7%
	-36	162	163	134	153	10.7%	0	125	372	166	114.3%	7.5%
K	-6	471	471	OL	471	0.0%	1004	OL	1122	1063	7.9%	55.7%
	-18	424	325	368	372	13.4%	462	635	433	510	21.5%	27.0%
	-30	267	299	338	301	11.8%	249	269	260	259	3.9%	16.2%
L	-6	764	794	791	783	2.1%	1109	1112	1441	1221	15.6%	35.9%
	-18	747	841	634	740	14.0%	737	805	650	731	10.6%	1.4%
	-30	204	431	300	311	36.6%	189	459	281	310	44.3%	0.5%
M	-12	OL	675	617	646	6.3%	OL	710	886	798	15.5%	19.0%
	-24	501	319	339	386	25.9%	440	453	611	501	18.9%	22.9%
	-36	332	419	224	325	30.1%	450	449	209	369	37.6%	12.0%

D = Difference (%) between Average of Method 1 and Method 2

$$= \frac{Ave_{method\,2} - Ave_{method\,1}}{Ave_{method\,2}} \times 100(\%)$$

TASK 2

In this task, IDT creep and strength testing and BBR creep testing of thin mixture beams were performed. The IDT tests were conducted at the same three temperatures as the SCB, with three replicates per temperature.

For IDT, two parameters, creep compliance and strength were determined using the current AASHTO specification T 322-03, "Standard Method of Test for Determining the Creep Compliance and Strength of Hot-Mix Asphalt (HMA) Using the Indirect Tensile Test Device." The IDT specimens were first tested for the creep stiffness and later for the strength. Both procedures are specified in AASHTO T 322-03 and the resultant parameters are calculated as follows:

- Creep stiffness:

$$D(t) = \frac{\Delta X \cdot D_{avg} \cdot b_{avg}}{P_{avg} \cdot GL} \cdot C_{cmpl}$$, where

$D(t)$ – creep compliance,
ΔX – trimmed mean of the horizontal deformations,
D_{avg} – average specimen diameter,
b_{avg} - average specimen thickness,
P_{avg} – average force during the test,
GL – gage length (38mm)
C_{cmpl} – creep compliance parameter at any given time, computed as

$$C_{cmpl} = 0.6354 \cdot \left(\frac{X}{Y} \right)^{-1} - 0.332$$, where

X – horizontal deformation,
Y – vertical deformation.

Creep stiffness $S(t)$ at the time t was calculated as the inverse of the creep compliance $D(t)$, i.e. $S(t)=1/D(t)$.

- Tensile strength:

$$S = \frac{2 \cdot P_{fail}}{\pi \cdot b \cdot D}$$, where

P_{fail} – failure (peak) load,
b, D – specimen thickness and diameter, respectively.

The AASHTO procedure leads to one value of the creep stiffness $S(t)$ for a given mixture at each temperature. An alternative method, referred to as the Zhang, Drescher and Newcomb method (ZDN) was also used based on work described elsewhere (Zofka 2008, Zhang et al. 1997).

For BBR, the thin mixture beams were cut from gyratory cylinders and then tested based on the method described in NCHRP Idea 133 (2009). The same three test temperatures used for SCB and IDT testing were used. Three replicates were tested at each temperature. Both IDT creep compliance and BRR creep compliance were converted to relaxation modulus values using Hopkins and Hamming interconversion method. The relaxation modulus was further used to calculate thermal stresses and intersect it with the IDT strength master curve. A summary of IDT strength values is given in Table 7 and Figures 7 and 8 show plots of the average values for the mixture tested. From Figures 9 to Figure 20 show the relaxation master curves and from Figures

21 to 32 show thermal stress curves using two different cooling rates plotted together with the IDT strength curve.

Table 7. Summary of mixture IDT strength results.

Mix ID	T °C	IDT Strength , MPa				
		R1	R2	R3	Average	CV (%)
A	-6	3.16	3.46	3.15	3.25	5.4%
	-18	4.78	4.67	4.42	4.62	4.0%
	-30	5.15	4.78	4.76	4.89	4.5%
B	-12	3.31	3.13	3.12	3.19	3.4%
	-24	4.46	4.20	4.15	4.27	3.9%
	-36	3.77	3.67	3.30	3.58	6.9%
D	-12	3.76	3.55	4.24	3.85	9.2%
	-24	6.27	4.74	6.10	5.70	14.7%
	-36	6.58	5.76	5.49	5.94	9.5%
E	-12	3.76	3.84	3.66	3.75	2.5%
	-24	4.92	4.43	5.17	4.84	7.8%
	-36	3.96	4.18	4.31	4.15	4.3%
F	-12	3.52	3.21	3.15	3.29	6.0%
	-24	3.57	4.31	3.90	3.93	9.3%
	-36	3.08	3.66	3.74	3.49	10.2%
G	-6	4.04	3.98	4.12	4.05	1.8%
	-18	4.44	4.51	4.24	4.40	3.3%
	-30	3.89	4.32	3.79	4.00	7.0%
H	-6	4.17	3.80	3.75	3.91	5.8%
	-18	4.12	4.52	5.01	4.55	9.8%
	-30	3.99	4.28	5.02	4.43	12.0%
I	-12	4.24	3.68	4.20	4.04	7.8%
	-24	4.31	4.97	4.93	4.74	7.8%
	-36	4.41	4.50	5.11	4.67	8.1%
J	-12	1.42	1.78	1.67	1.62	11.4%
	-24	2.53	2.13	1.99	2.21	12.6%
	-36	2.16	1.83	1.53	1.84	17.1%
K	-6	3.07	3.21	NA	3.14	3.2%
	-18	4.32	3.39	4.03	3.91	12.2%
	-30	3.98	3.30	3.64	3.64	9.4%
L	-12	4.41	3.95	3.72	4.03	8.6%
	-24	4.30	4.73	4.05	4.36	7.9%
	-36	4.77	4.67	4.16	4.53	7.2%
M	-6	3.58	3.81	3.94	3.78	4.8%
	-18	4.98	4.42	4.22	4.54	8.7%
	-30	4.57	3.89	3.65	4.03	11.9%

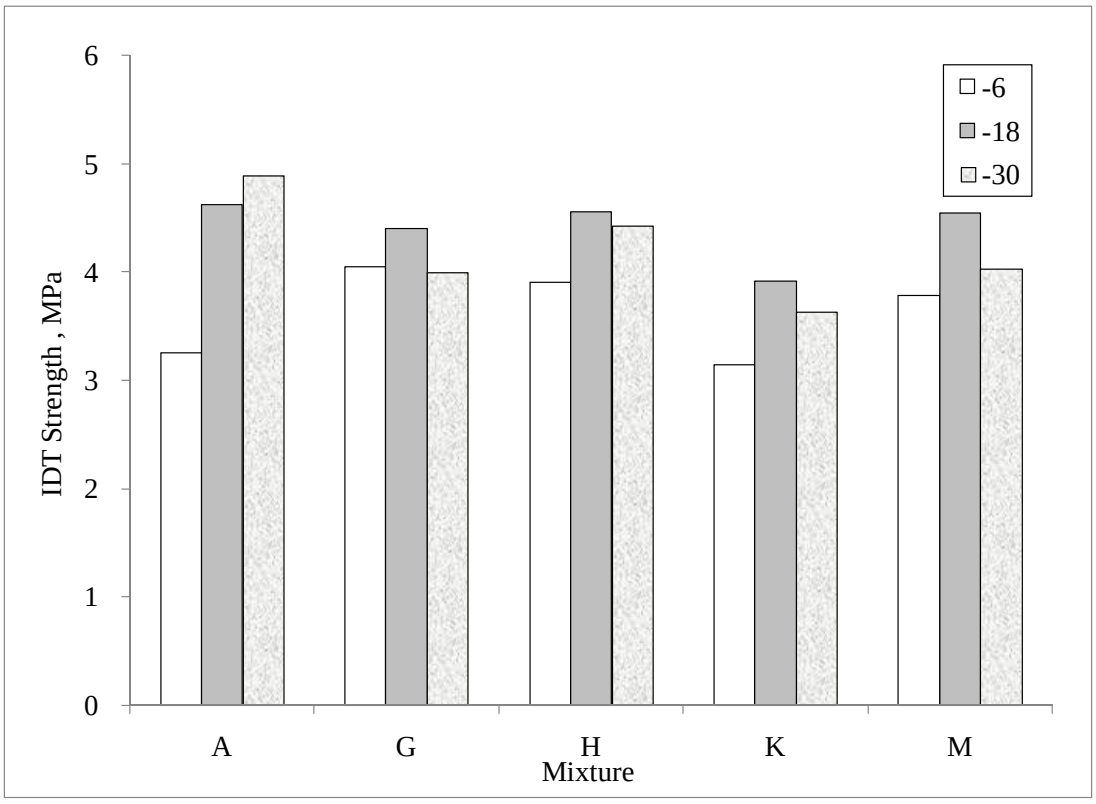

Figure 7. IDT strength values (mixtures A, G, H, K, M)

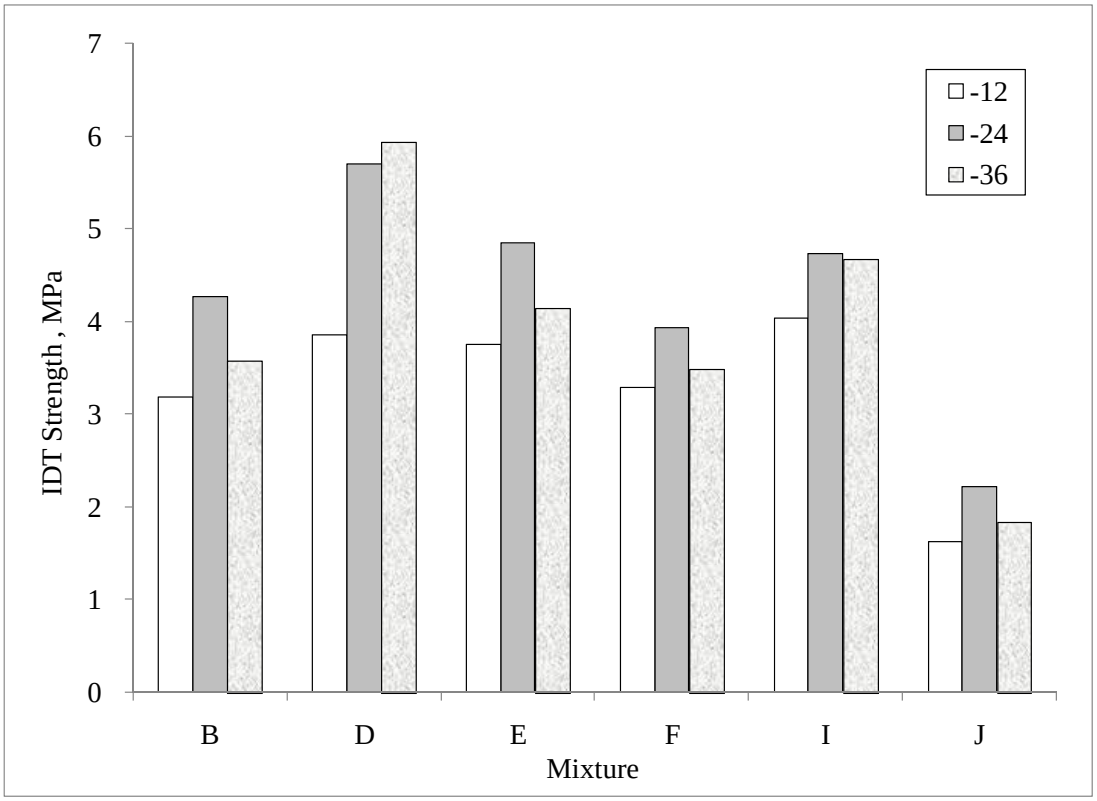

Figure 8. IDT strength values (mixtures B, D, E, F, I, J)

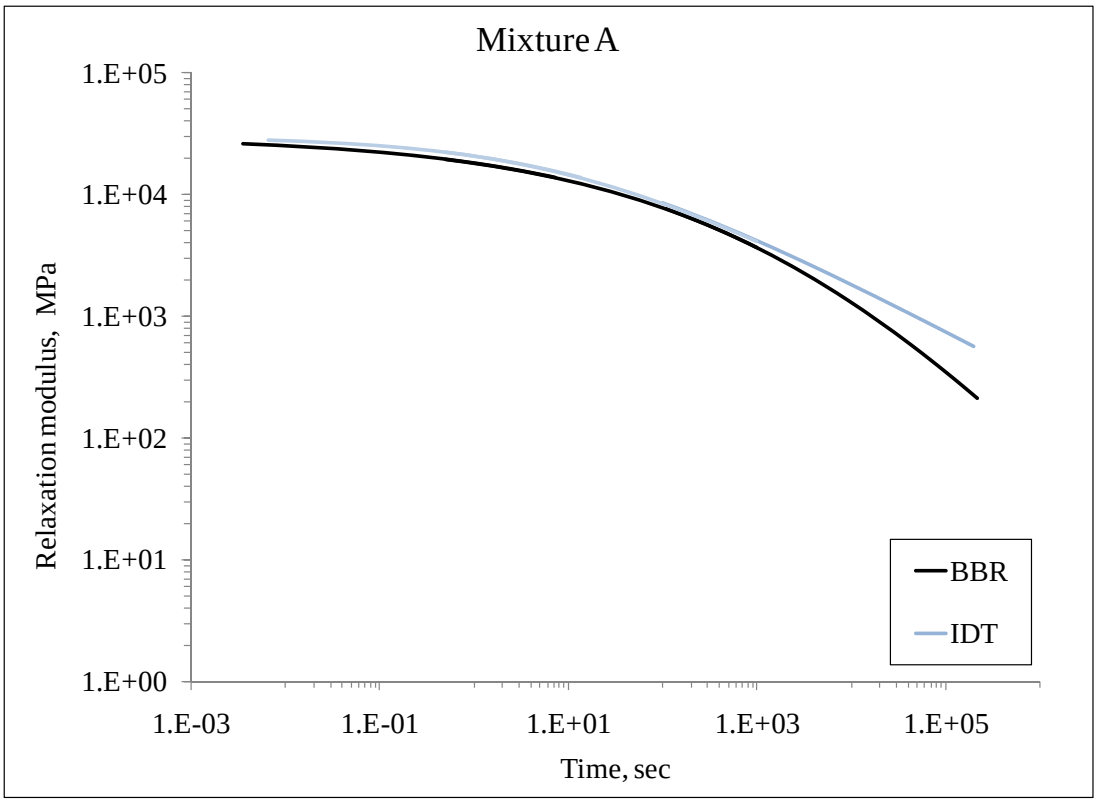

Figure 9. Relaxation modulus mastercurve at -18°C, mixture A

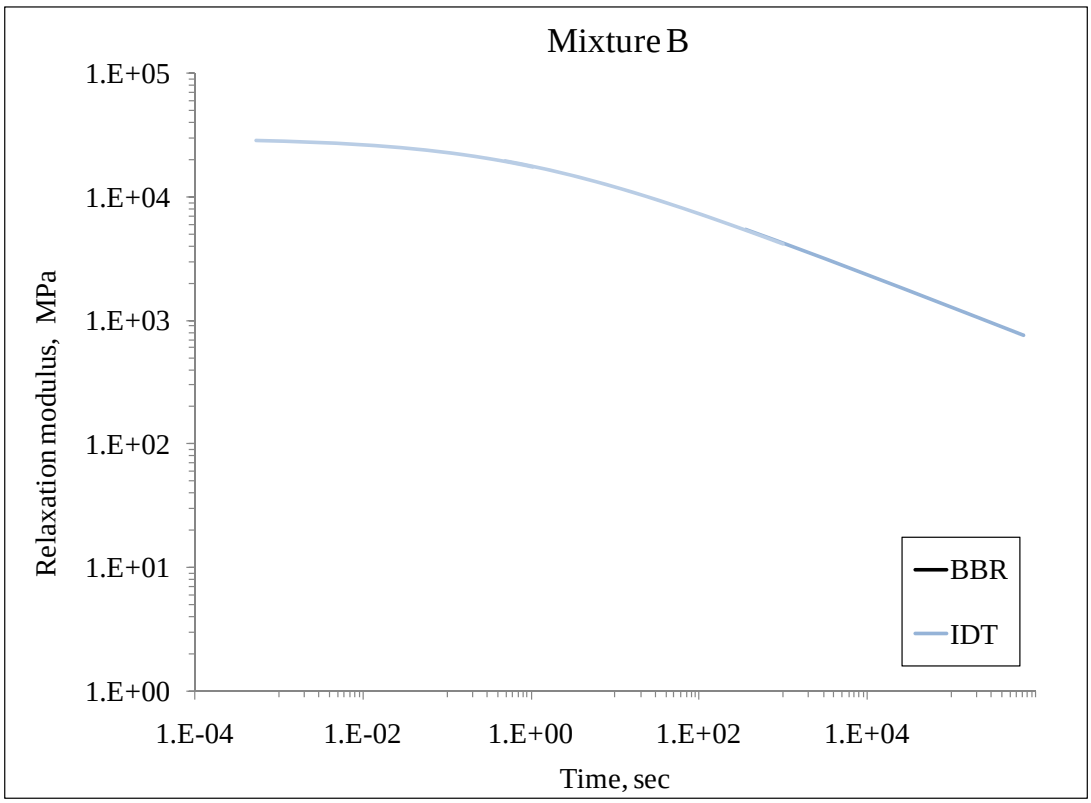

Figure 10. Relaxation modulus mastercurve at -24°C, mixture B

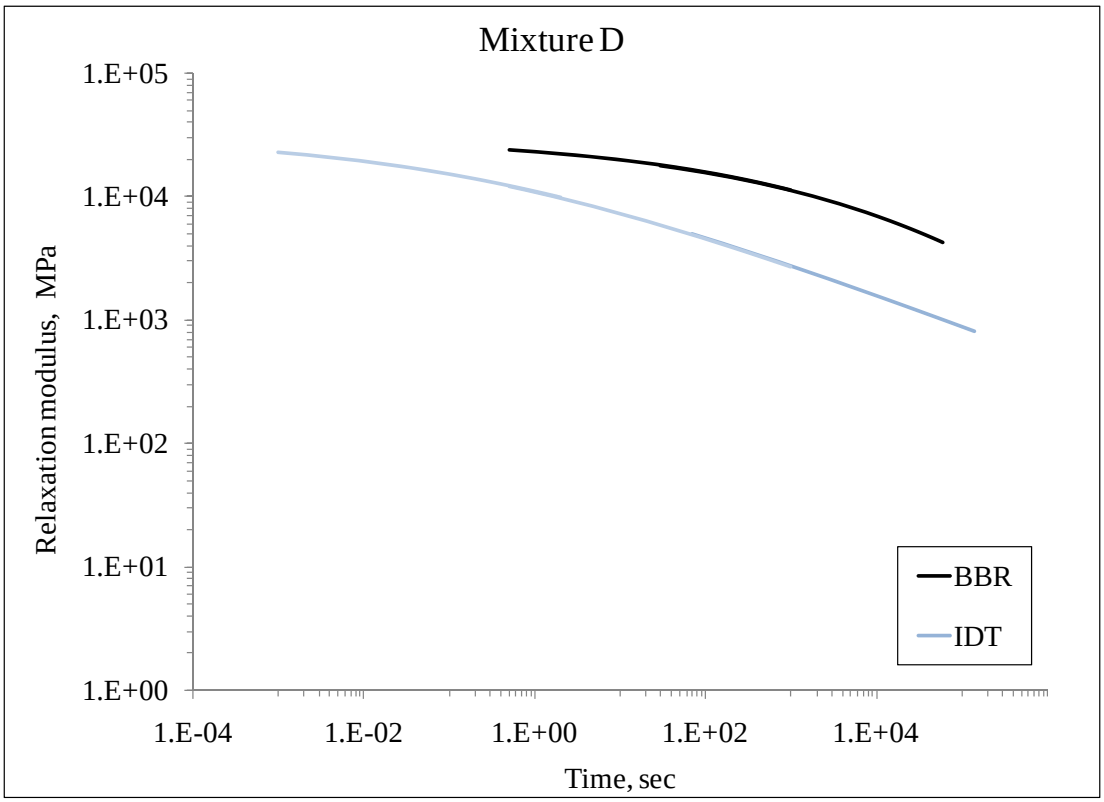

Figure 11. Relaxation modulus mastercurve at -24°C, mixture D

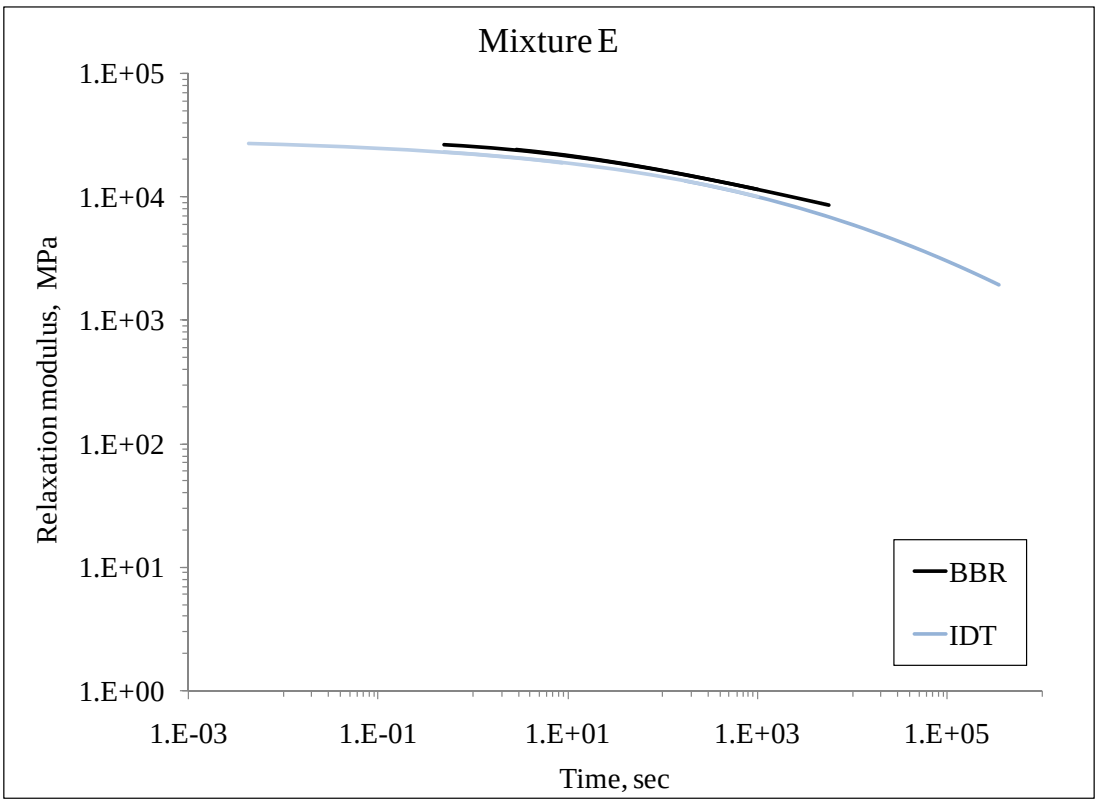

Figure 12. Relaxation modulus mastercurve at -24°C, mixture E

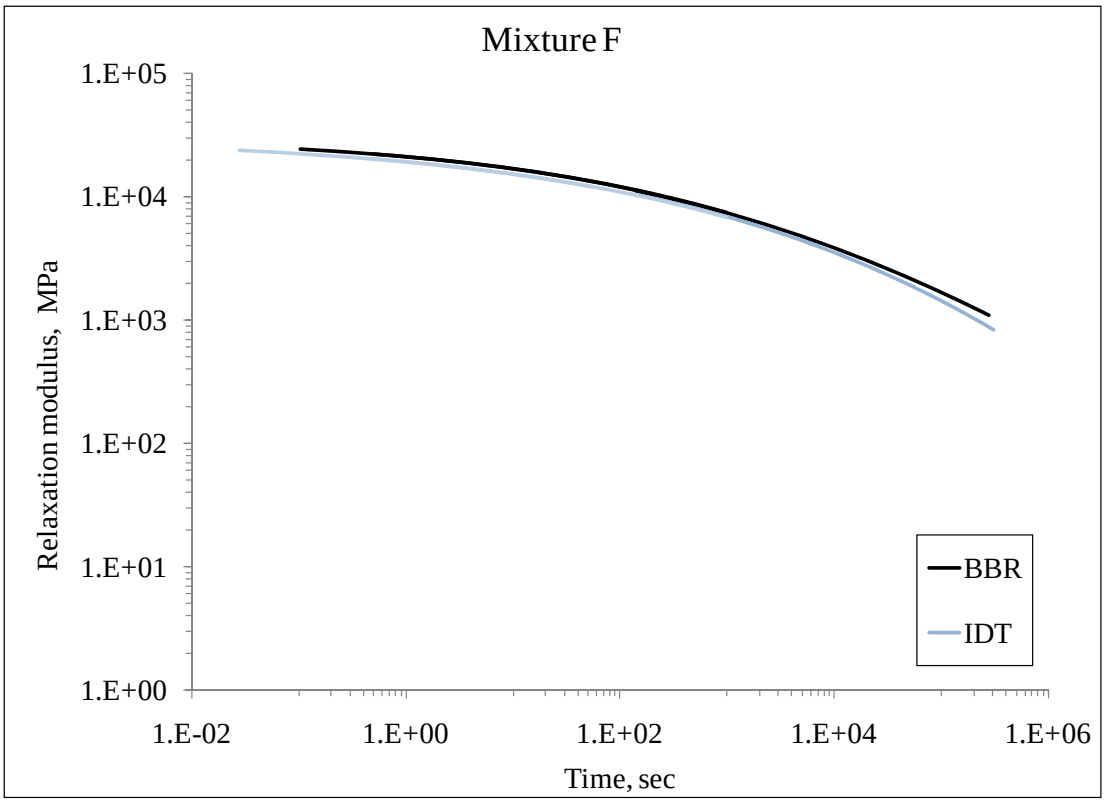

Figure 13. Relaxation modulus mastercurve at -24°C, mixture F

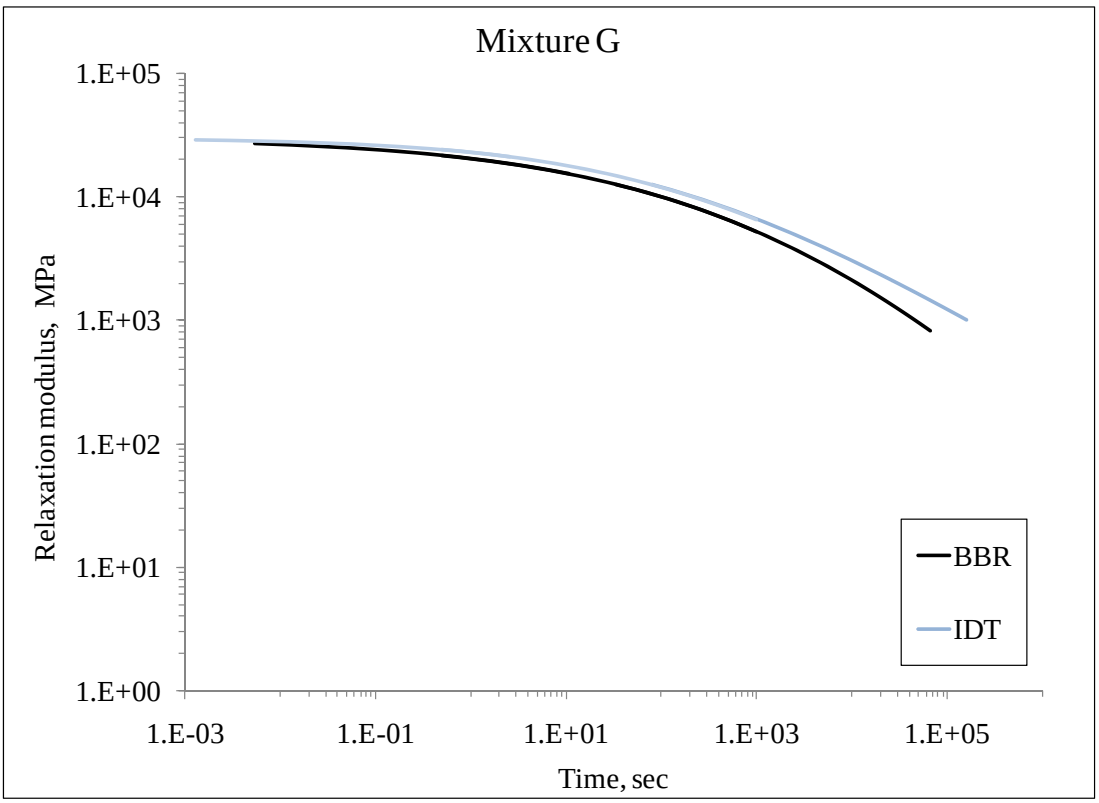

Figure 14. Relaxation modulus mastercurve at -18°C, mixture G

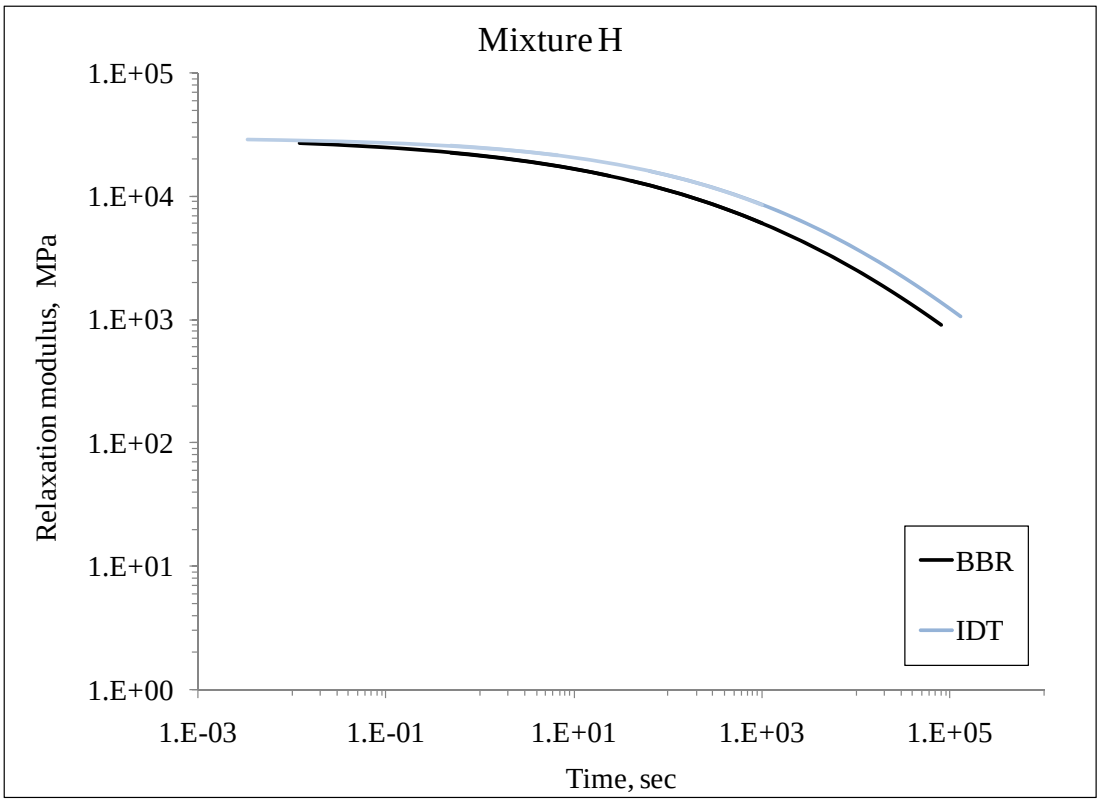

Figure 15. Relaxation modulus mastercurve at -18°C, mixture H

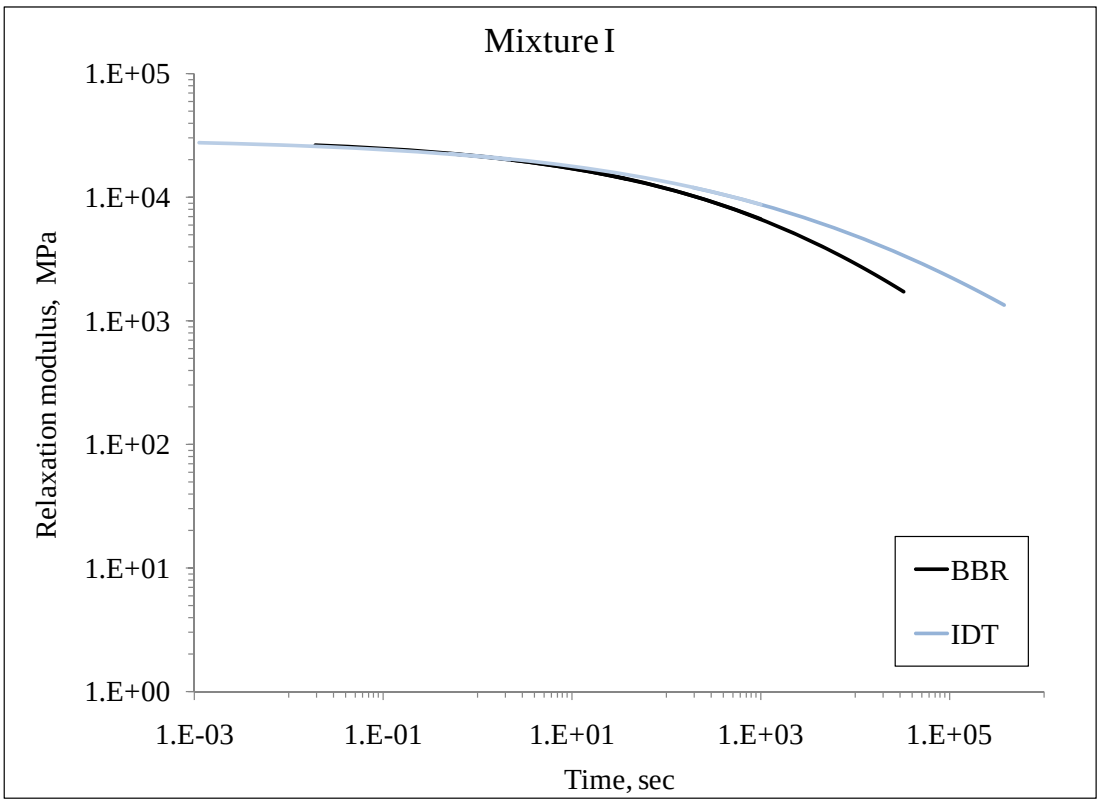

Figure 16. Relaxation modulus mastercurve at -24°C, mixture I

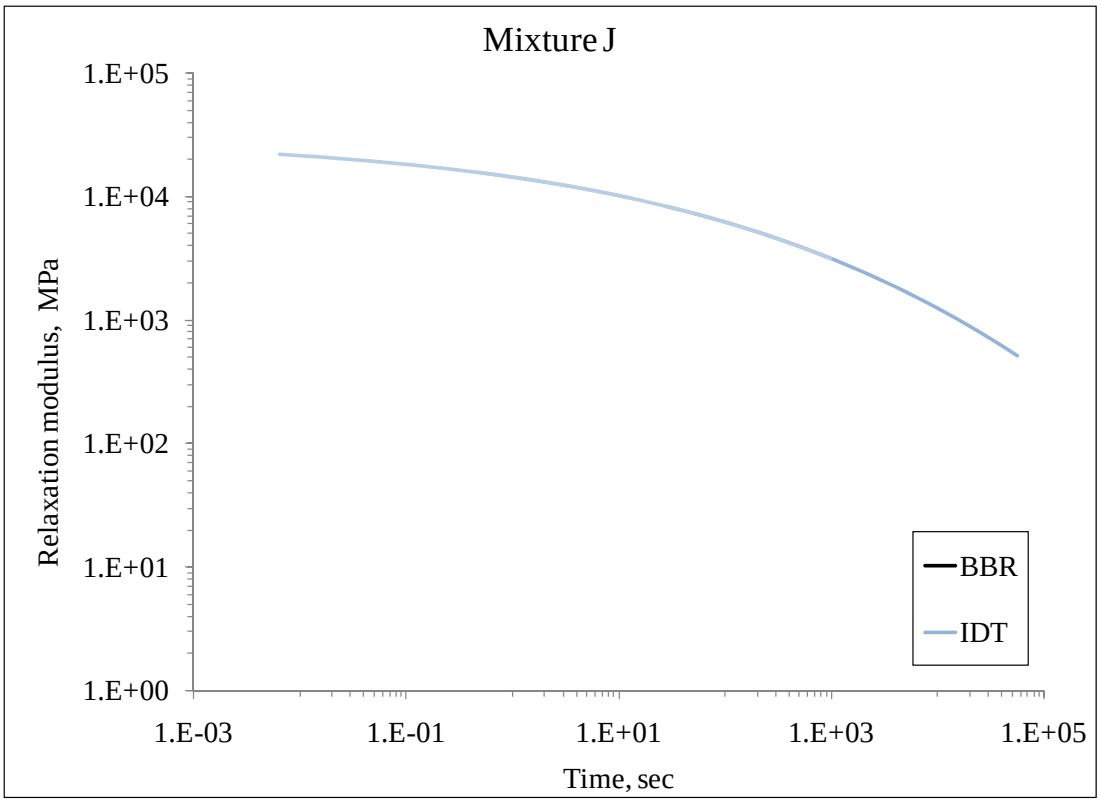

Figure 17. Relaxation modulus mastercurve at -24°C, mixture J

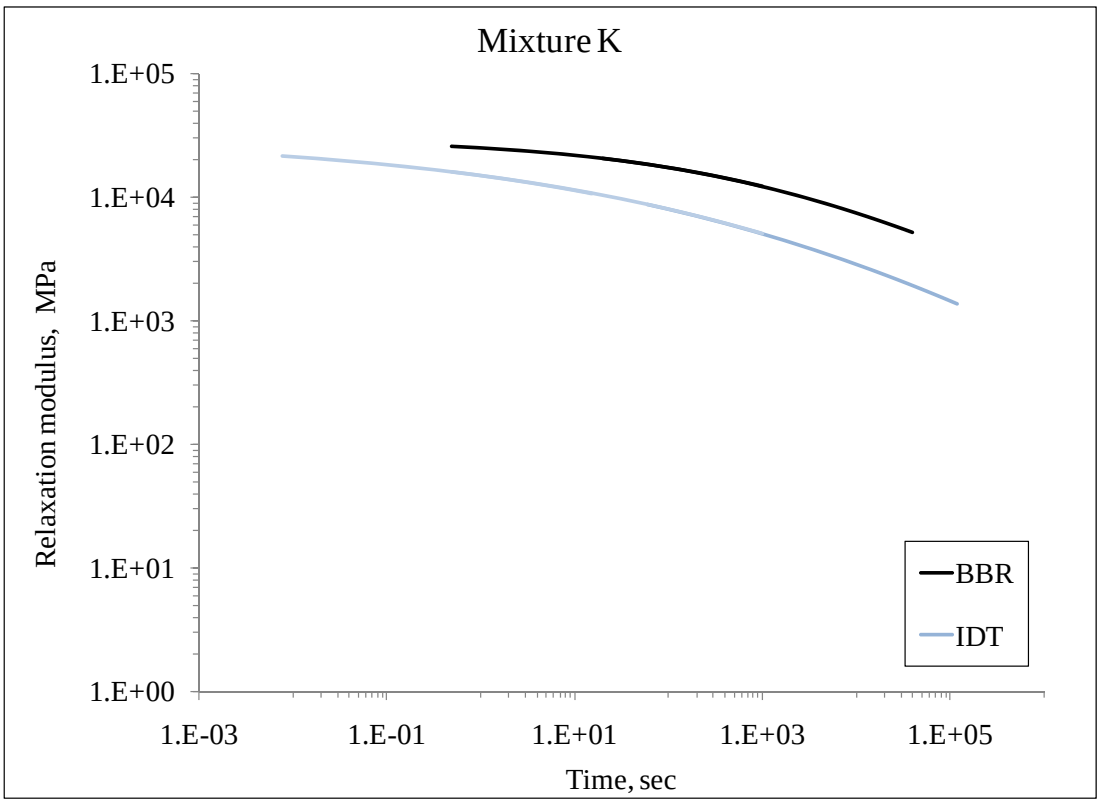

Figure 18. Relaxation modulus mastercurve at -24°C, mixture K

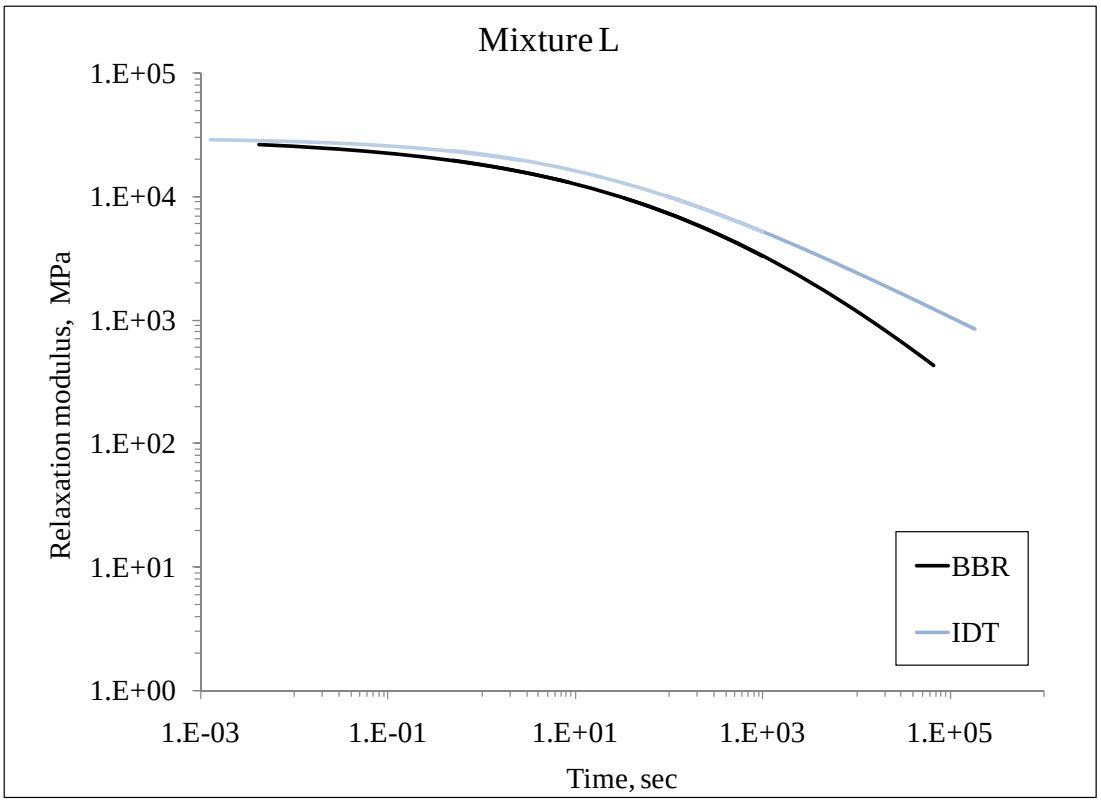

Figure 19. Relaxation modulus mastercurve at -24°C, mixture L

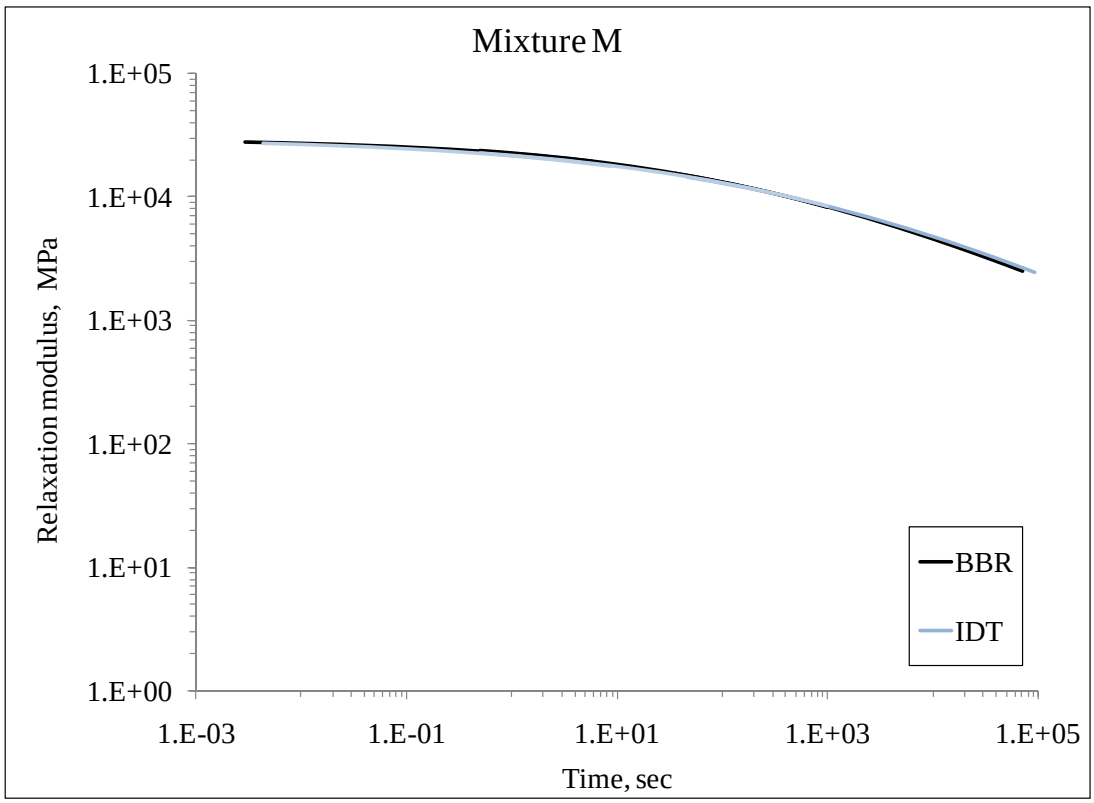

Figure 20. Relaxation modulus mastercurve at -18°C, mixture M

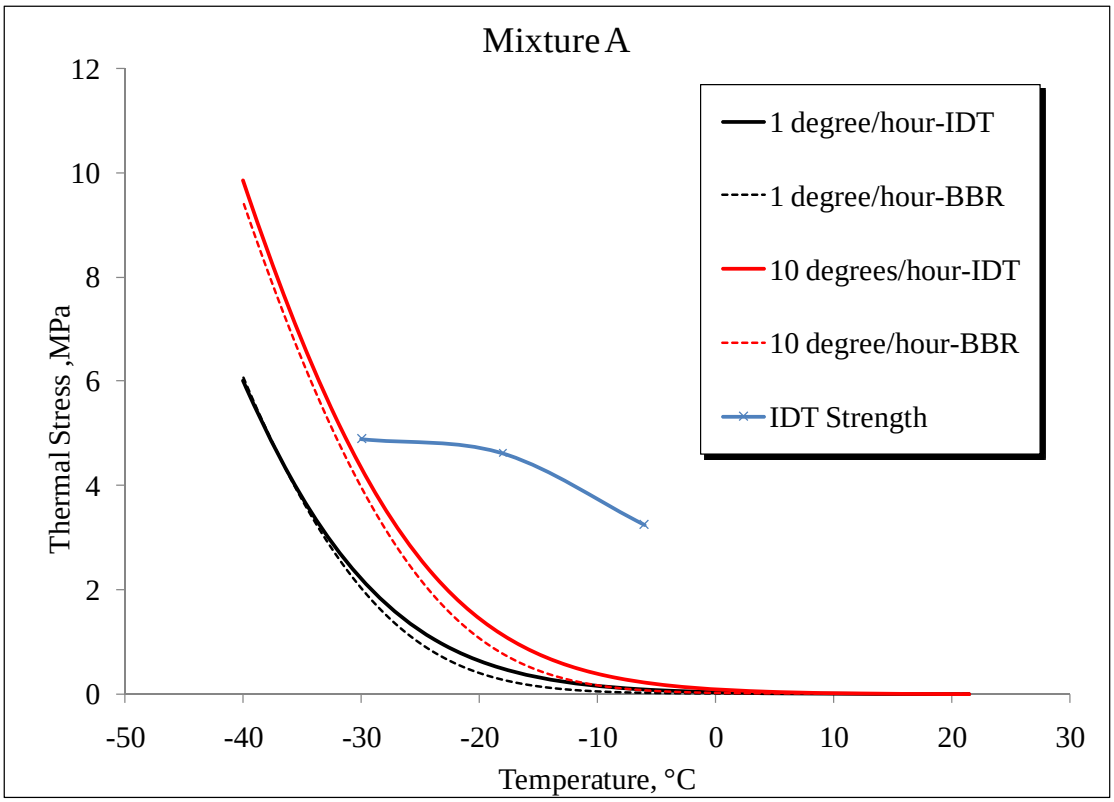

Figure 21. Thermal stress calculation for mixture A

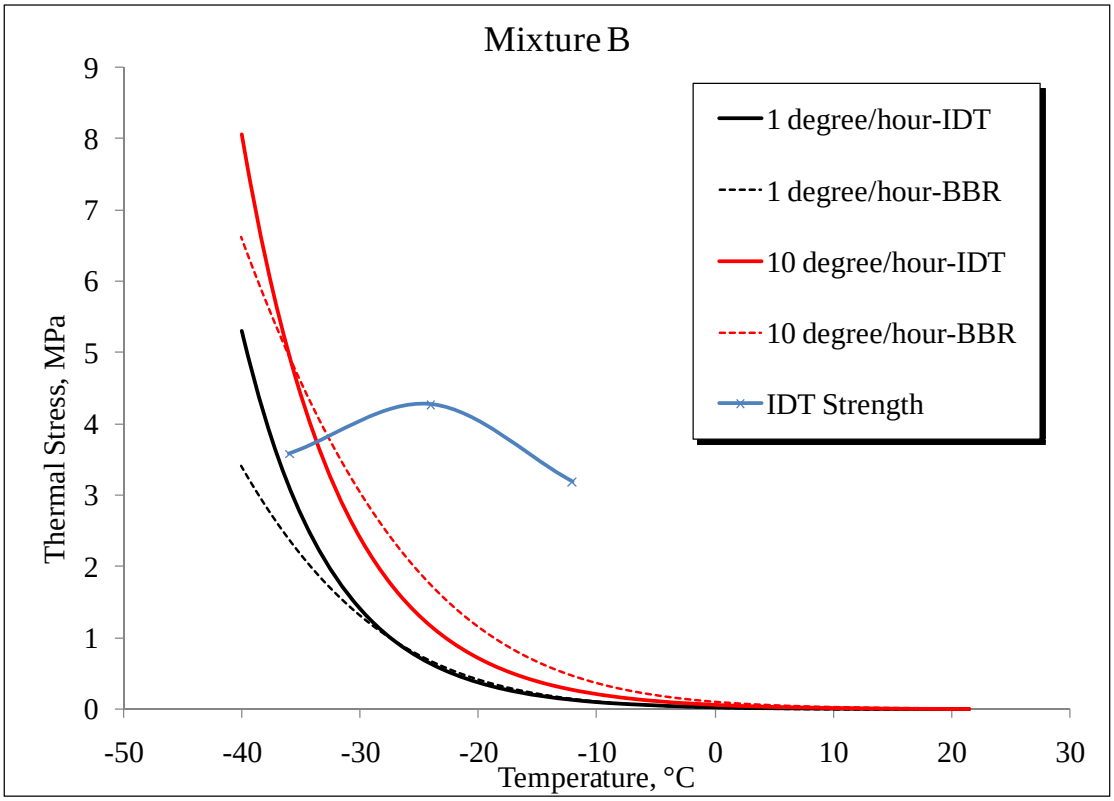

Figure 22. Thermal stress calculation for mixture B

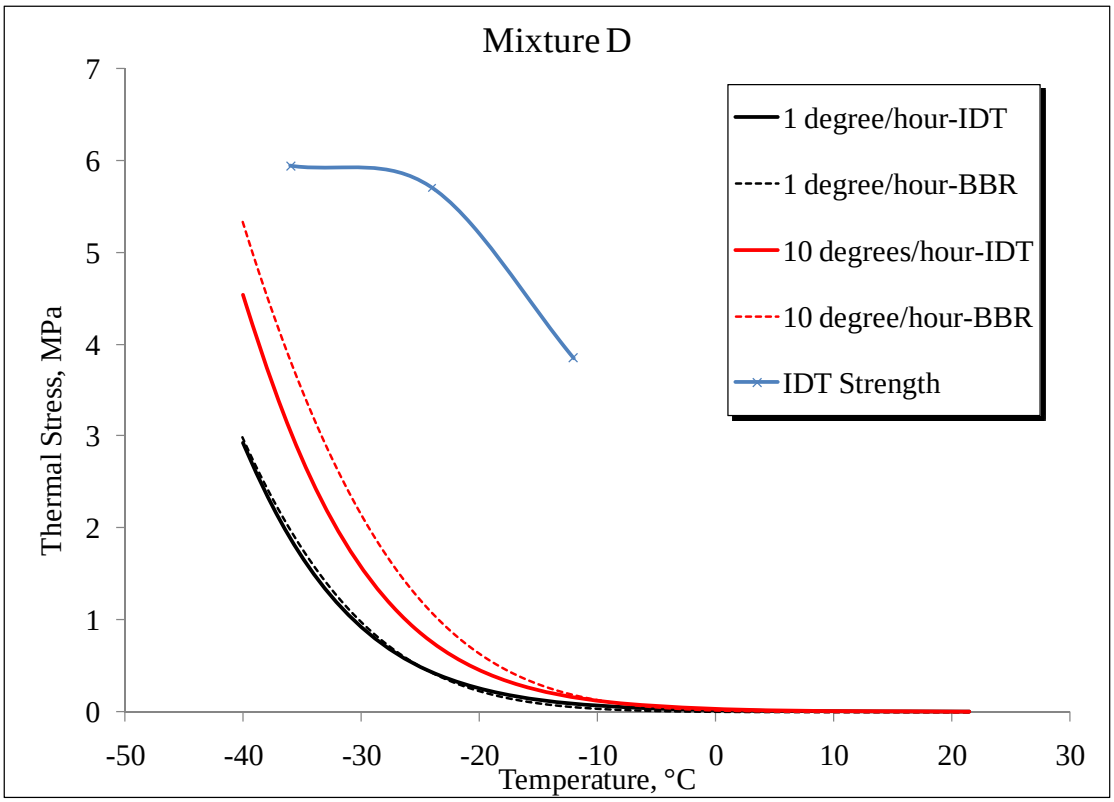

Figure 23. Thermal stress calculation for mixture D

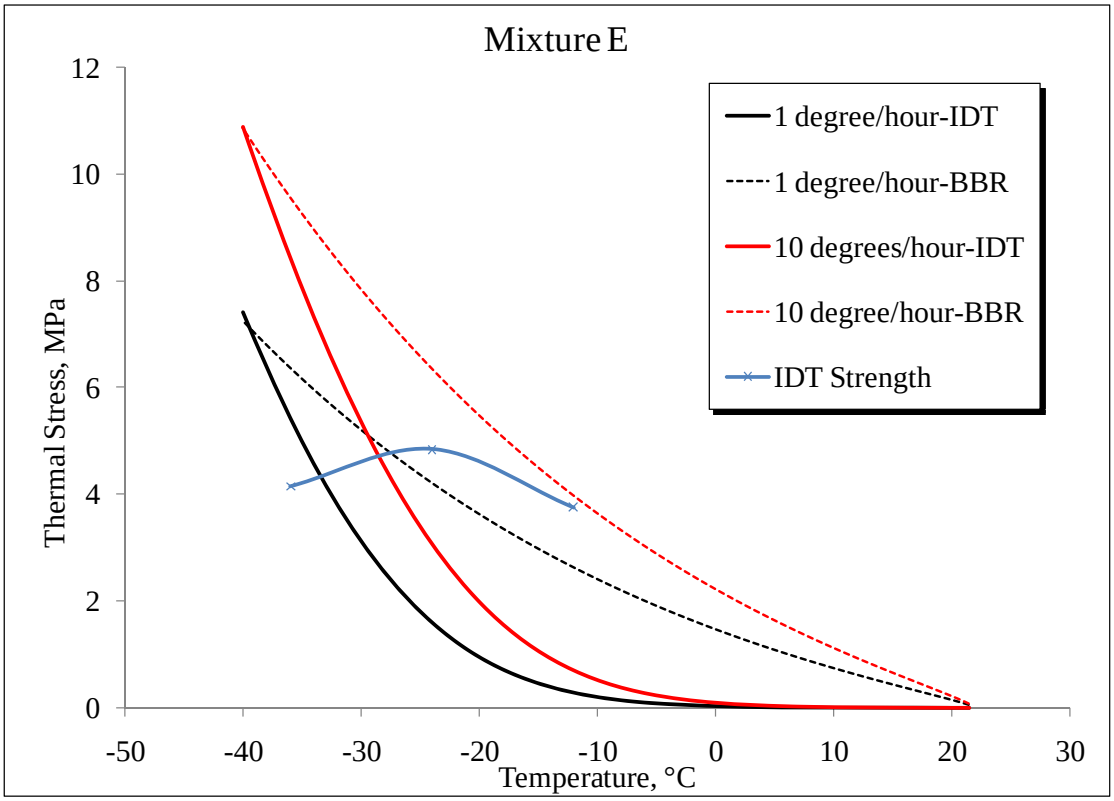

Figure 24. Thermal stress calculation for mixture E

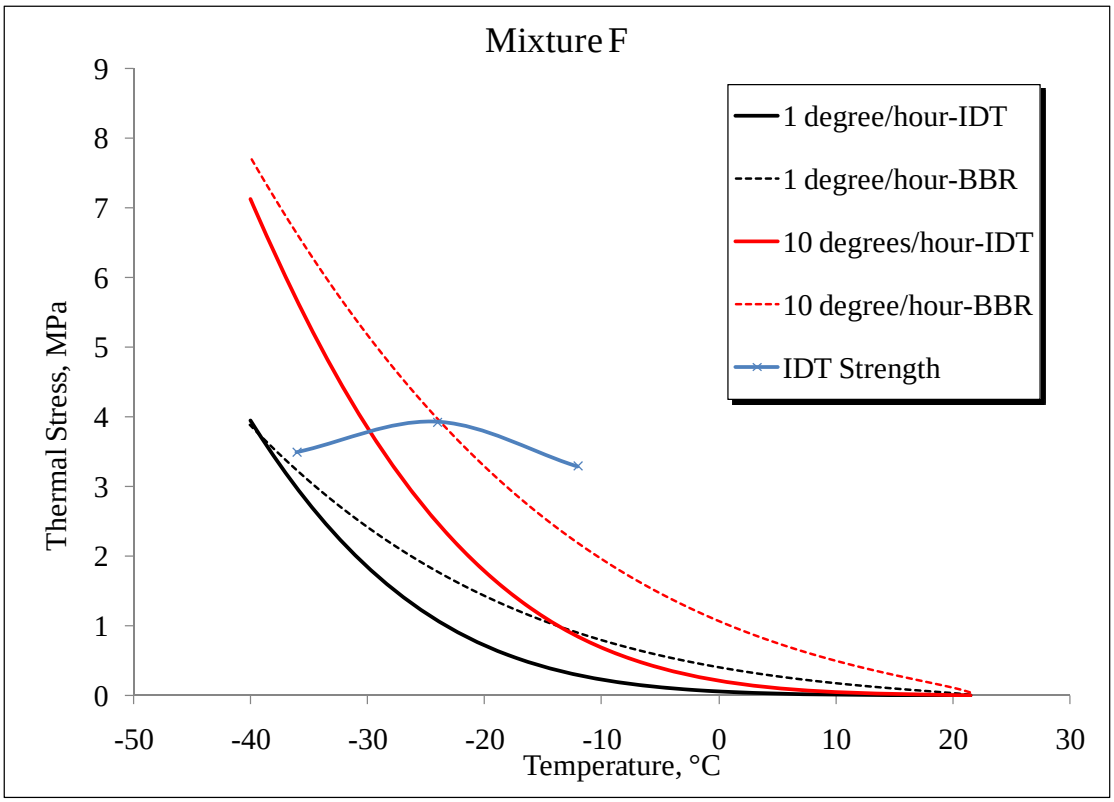

Figure 25. Thermal stress calculation for mixture F

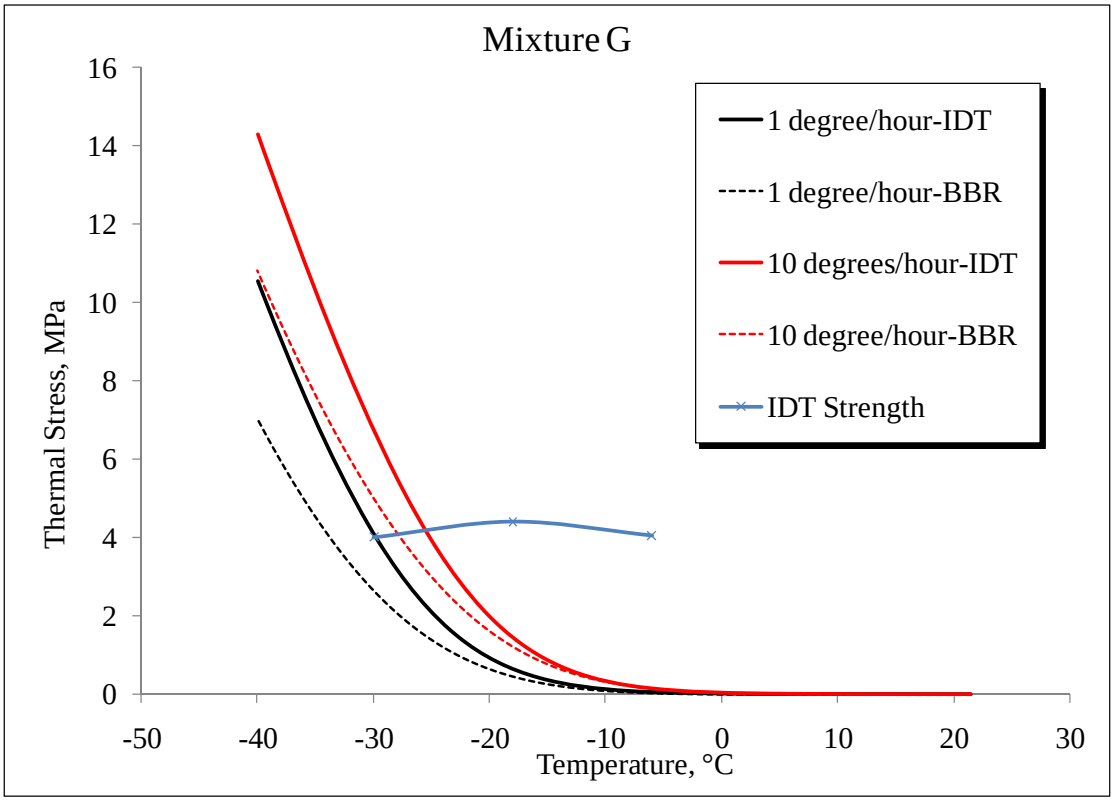

Figure 26. Thermal stress calculation for mixture G

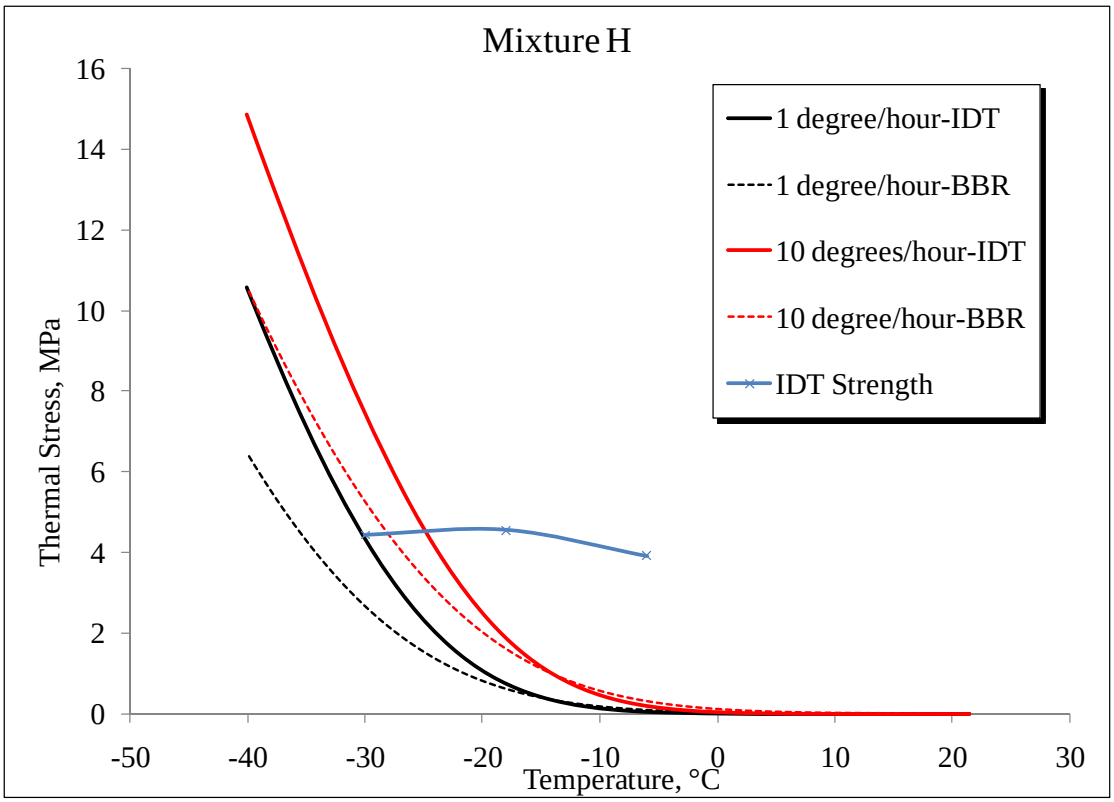

Figure 27. Thermal stress calculation for mixture H

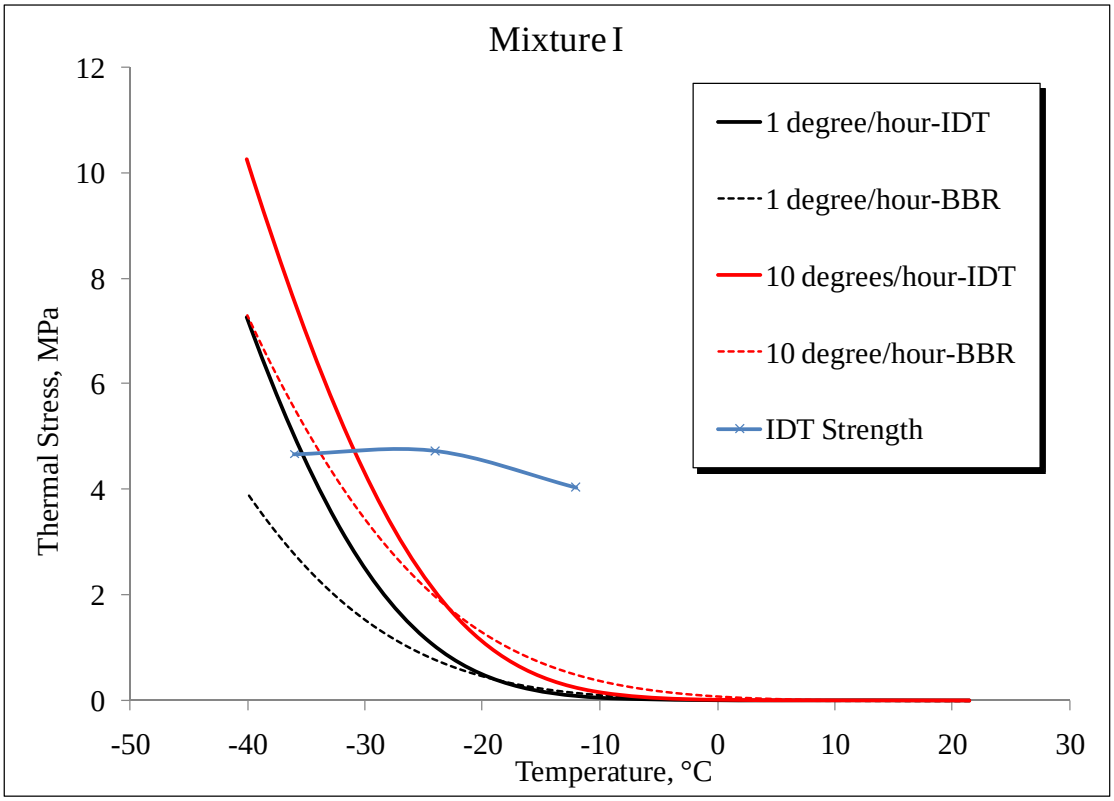

Figure 28. Thermal stress calculation for mixture I

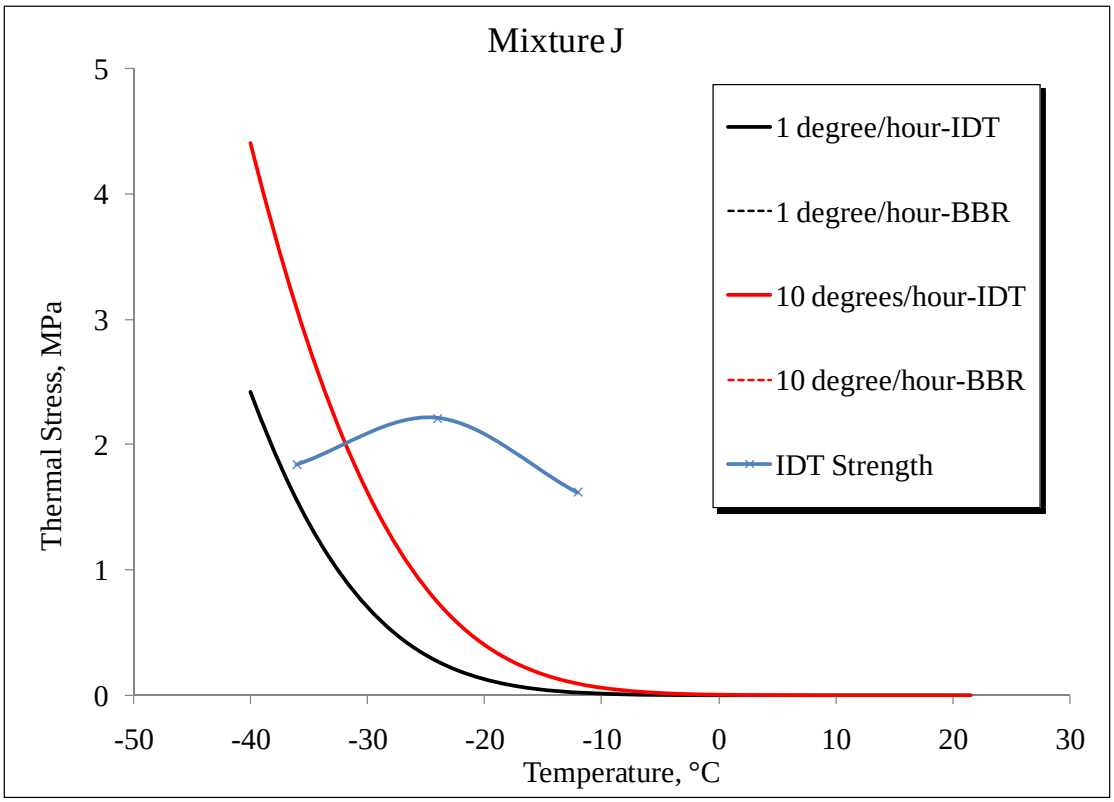

Figure 29. Thermal stress calculation for mixture J

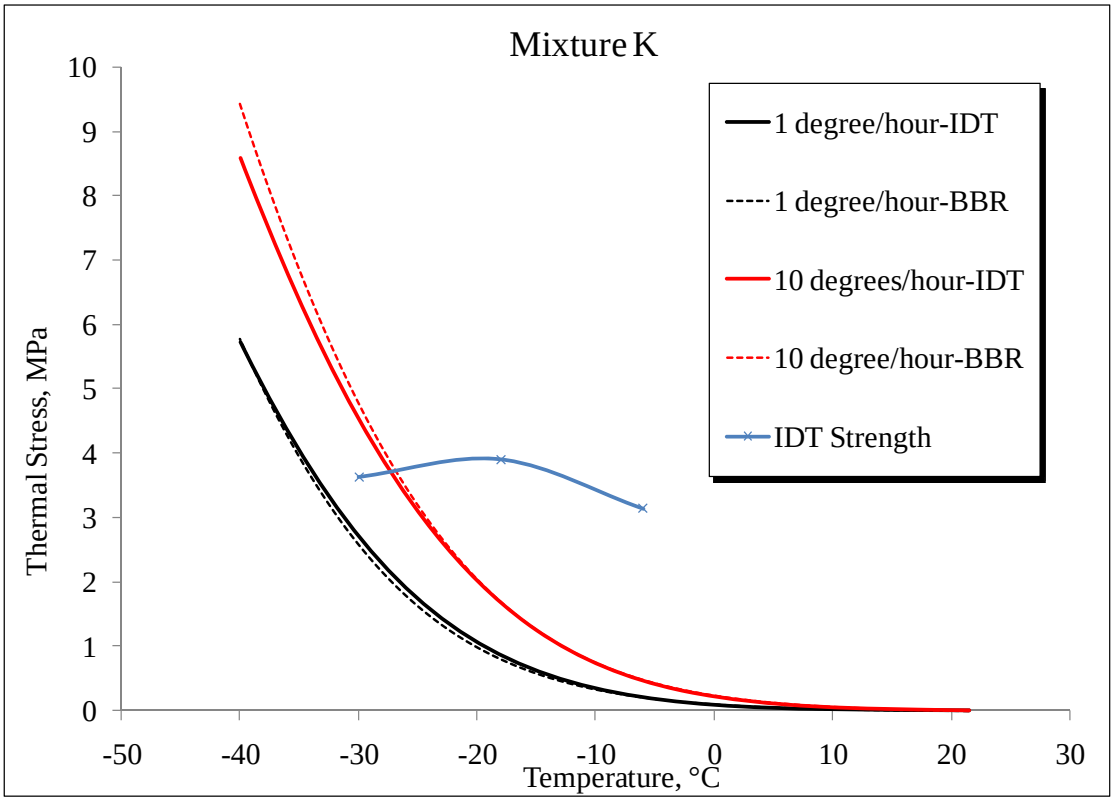

Figure 30. Thermal stress calculation for mixture K

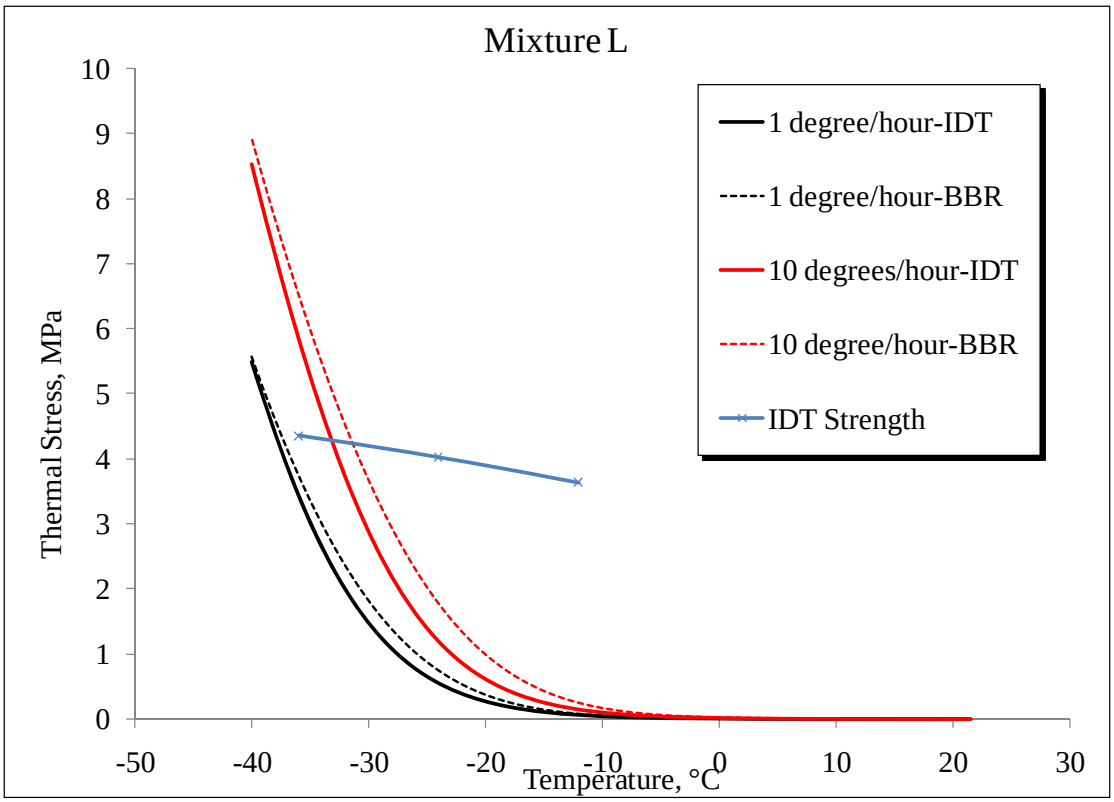

Figure 31. Thermal stress calculation for mixture L

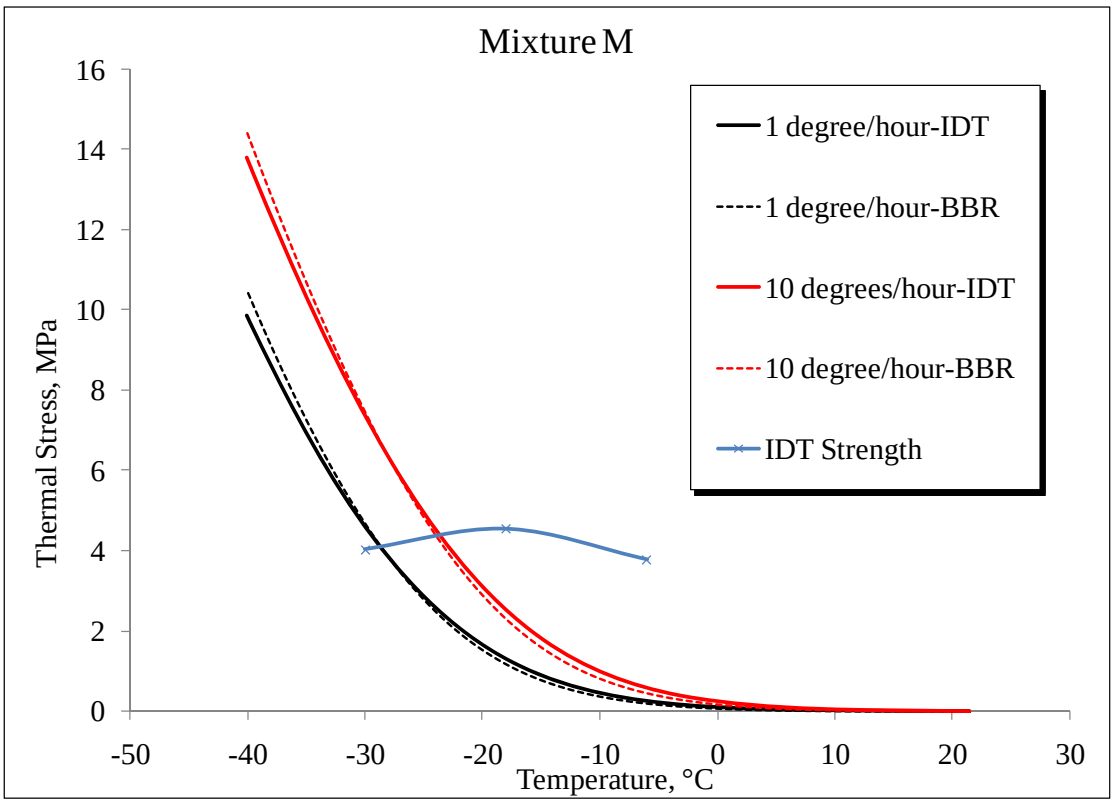

Figure 32. Thermal stress calculation for mixture M

TASK 3

In this task, direct tension (DT) and double edge notch tension (DENT) tests were performed on the PAV and extracted asphalt binders described in Table 2. The DT tests were conducted at two temperatures, PG + 10°C and PG + 4°C; three to six replicates were tested at each temperature depending on how much material was available.

To further investigate low-temperature fracture behavior of the asphalt binders, DENT tests were also performed at the same temperatures using the procedure described elsewhere (Zofka and Marasteanu 2007). A razor blade was used to make 1.5mm pre-cracks on both sides of the test specimens and a strain rate was 1%/min was used. Asphalt binder mode I critical stress intensity factor (fracture toughness) K_{IC} was calculated using the following equation:

$$K_{IC} = \frac{P}{B\sqrt{W}} \frac{\sqrt{\frac{\pi a}{2W}}}{\sqrt{1-\frac{a}{W}}} \left[1.122 - 0.561\left(\frac{a}{W}\right) - 0.205\left(\frac{a}{W}\right)^2 + 0.471\left(\frac{a}{W}\right)^3 + 0.190\left(\frac{a}{W}\right)^4 \right]$$

where:

P – peak load [kN],
B – specimen thickness [mm]
W – half width of the specimen [mm],
a – length of the notch and pre-crack [mm].

An example of stress strain curves obtained from the Direct Tension data is shown in Figure 33. Summaries of the results obtained with the two test methods are shown in Tables 8 to 12.

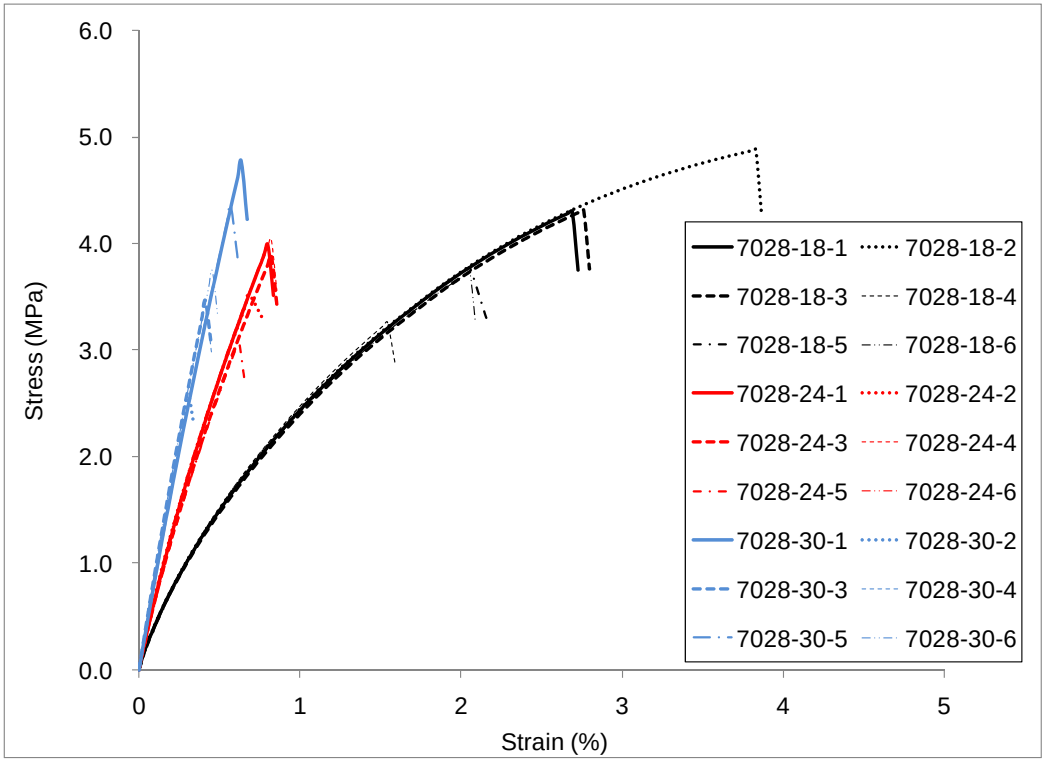

Figure 33. DTT stress-strain curves for asphalt binder PG64-22

Table 8. Summary of asphalt binders DTT strength results.

Binder ID	T °C	DTT Strength , MPa					CV(%)
		R1	R2	R3	R4	Ave	
21-Fine	-18	4.29	3.98	3.44	3.17	3.72	13.7%
	-24	5.07	4.23	3.67	3.48	4.11	17.4%
	-30	4.67	3.79	1.75	1.34	2.89	55.6%
21-Coarse	-18	5.85	5.75	3.98	3.32	4.72	26.9%
	-24	4.94	4.46	4.44	2.48	4.08	26.8%
	-30	3.57	2.62	2.28	2.27	2.68	22.7%
21-Standard	-18	5.11	4.95	4.85	1.91	4.20	36.5%
	-24	6.26	6.13	6.00	4.64	5.76	13.1%
	-30	5.63	3.60	3.05	1.97	3.56	43.0%
PG-58-28	-18	3.68	3.65	3.61	3.57	3.63	1.2%
	-24	5.18	4.44	4.17	4.14	4.48	10.9%
	-30	4.52	4.23	3.97	3.87	4.15	7.0%
PG-58-34	-24	5.34	4.44	4.26	4.12	4.54	12.1%
	-30	5.14	5.08	5.05	4.59	4.97	5.1%
PG-58-34W	-24	3.93	3.90	3.58	3.47	3.72	6.1%
	-30	4.19	4.17	3.70	3.51	3.89	8.9%
PG-64-22	-12	4.85	4.05	3.16	2.91	3.74	23.6%
	-18	4.59	4.40	4.38	4.08	4.36	4.8%
	-24	4.28	3.49	2.90	2.82	3.37	20.0%
PG-64-34	-24	5.12	4.64	4.16	4.11	4.51	10.5%
	-30	5.37	5.36	4.89	4.84	5.12	5.7%
PG-70-28	-18	4.82	4.33	4.31	3.83	4.32	9.3%
	-24	4.32	4.32	4.30	4.16	4.28	1.9%
	-30	5.22	4.82	4.25	3.97	4.57	12.3%

Table 9. Summary of asphalt binders DTT strain at failure results.

Binder ID	T °C	DTT Strain at failure , %					CV(%)
		R1	R2	R3	R4	Ave	
21-Fine	-18	1.23	1.04	0.95	0.81	1.01	17.6%
	-24	0.92	0.69	0.58	0.55	0.69	24.6%
	-30	0.53	0.40	0.17	0.13	0.31	63.3%
21-Coarse	-18	2.85	2.57	2.48	1.04	2.23	36.5%
	-24	0.95	0.86	0.81	0.40	0.76	32.2%
	-30	0.40	0.30	0.25	0.23	0.30	25.7%
21-Standard	-18	2.18	2.00	1.95	0.49	1.65	47.5%
	-24	1.30	1.30	1.23	0.83	1.17	19.2%
	-30	0.69	0.40	0.32	0.21	0.41	50.1%
PG-58-28	-18	1.35	1.30	1.35	1.25	1.31	3.6%
	-24	0.90	0.76	0.67	0.69	0.75	13.5%
	-30	0.48	0.44	0.42	0.40	0.44	8.4%
PG-58-34	-24	2.65	1.95	1.77	1.75	2.03	20.8%
	-30	1.00	1.03	0.90	0.86	0.95	8.3%
PG-58-34W	-24	1.58	1.48	1.36	1.26	1.42	9.8%
	-30	0.74	0.75	0.63	0.55	0.67	14.0%
PG-64-22	-12	3.94	2.42	1.53	1.36	2.31	51.0%
	-18	0.95	0.91	0.88	0.82	0.89	6.5%
	-24	0.49	0.40	0.29	0.29	0.37	25.9%
PG-64-34	-24	3.99	3.30	2.24	1.91	2.86	33.6%
	-30	1.14	1.12	1.03	0.93	1.06	9.2%
PG-70-28	-18	4.01	2.89	2.81	2.16	2.97	25.9%
	-24	0.89	0.87	0.87	0.89	0.88	1.6%
	-30	0.70	0.63	0.52	0.47	0.58	17.9%

Table 10. Summary of asphalt binders DENT strength results.

Binder ID	T °C	DENT Strength , MPa				CV %
		R1	R2	R3	Ave	
21-Fine	-18	0.62	0.59	0.54	0.58	6.9%
	-24	0.68	0.67	0.56	0.64	10.3%
21-Coarse	-18	0.57	0.46	0.44	0.49	14.1%
	-24	0.97	0.57	0.47	0.67	39.3%
21-Standard	-18	0.54	0.47	0.39	0.47	16.7%
	-24	0.70	0.61	0.46	0.59	20.0%
PG-58-28	-18	0.68	0.52	0.46	0.55	20.8%
	-24	0.78	0.71	0.70	0.73	5.9%
PG-58-34	-24	1.09	1.08	1.04	1.07	2.3%
	-30	0.99	0.82	0.61	0.81	23.7%
PG-58-34W	-24	0.91	0.90	0.84	0.88	4.3%
	-30	1.16	0.84	0.64	0.88	29.7%
PG-64-22	-12	0.85	0.80	0.76	0.80	5.6%
	-18	0.43	0.36	NA	0.39	14.0%
PG-64-34	-24	1.83	1.42	1.14	1.46	23.8%
	-30	1.42	1.39	1.31	1.38	4.3%
PG-70-28	-18	1.79	1.75	1.57	1.70	6.9%
	-24	1.44	1.27	1.07	1.26	14.9%

Table 11. Summary of asphalt binders DENT strain at failure results.

Binder ID	T °C	DENT Strain at failure , %				CV %
		R1	R2	R3	Ave	
21-Fine	-18	0.07	0.07	0.07	0.07	5.5%
	-24	0.06	0.06	0.05	0.05	7.8%
21-Coarse	-18	0.08	0.06	0.08	0.08	19.1%
	-24	0.11	0.06	0.04	0.07	49.1%
21-Standard	-18	0.07	0.06	0.05	0.06	18.5%
	-24	0.08	0.06	0.04	0.06	29.8%
PG-58-28	-18	0.10	0.06	0.06	0.07	29.6%
	-24	0.06	0.06	0.06	0.06	6.3%
PG-58-34	-24	0.17	0.20	0.16	0.17	12.3%
	-30	0.08	0.07	0.05	0.07	26.5%
PG-58-34W	-24	0.15	0.15	0.13	0.14	8.8%
	-30	0.11	0.08	0.06	0.08	30.6%
PG-64-22	-12	0.18	0.15	0.15	0.16	8.4%
	-18	0.04	0.03	NA	0.03	12.9%
PG-64-34	-24	0.45	0.27	0.21	0.31	41.6%
	-30	0.14	0.13	0.14	0.14	4.0%
PG-70-28	-18	0.48	0.44	0.38	0.43	12.1%
	-24	0.17	0.13	0.11	0.13	22.4%

Table 12. Summary of asphalt binders DENT K_{IC} results.

Binder ID	T °C	K_{IC} (Stress intensity factor) , kPa/$m^{0.5}$				CV %
		R1	R2	R3	Ave	
21-Fine	-18	103.1	98.3	89.9	97.1	6.9%
	-24	113.7	111.8	93.7	106.4	10.4%
21-Coarse	-18	95.0	76.0	74.0	81.7	14.2%
	-24	161.7	94.9	78.7	111.8	39.4%
21-Standard	-18	90.3	79.3	64.4	78.0	16.7%
	-24	116.8	102.4	77.5	98.9	20.1%
PG-58-28	-18	113.3	86.2	76.4	92.0	20.8%
	-24	130.0	117.9	117.5	121.8	5.8%
PG-58-34	-24	182.1	179.6	174.3	178.7	2.2%
	-30	165.6	136.9	101.9	134.8	23.7%
PG-58-34W	-24	151.5	149.6	139.7	146.9	4.3%
	-30	193.2	141.0	106.5	146.9	29.7%
PG-64-22	-12	141.3	133.1	126.2	133.5	5.7%
	-18	72.3	59.3	NA	65.8	14.0%
PG-64-34	-24	306.1	237.0	190.5	244.5	23.8%
	-30	237.8	233.0	218.9	229.9	4.3%
PG-70-28	-18	299.7	292.0	262.5	284.7	6.9%
	-24	241.0	212.4	178.6	210.6	14.8%

REFERENCES

1. American Association of State Highway and Transportation Officials (AASHTO) Standard T314-07, “Standard method of test for determining the fracture properties of asphalt binder in Direct Tension (DT),” *Standard Specifications for Transportation Materials and Methods of Sampling and Testing*, 27th Edition, 2007.
2. American Association of State Highway and Transportation Officials (AASHTO) Standard T 322-03, "Determining the Creep Compliance and Strength of Hot-Mix Asphalt (HMA) Using the Indirect Tensile Test Device", *Standard Specifications for Transportation Materials and Methods of Sampling and Testing*, 27th Edition, 2007.
3. Marasteanu, M., Velasquez, R., Falchetto, A.C., Zofka, A., *Development of a Simple Test to Determine the Low Temperature Creep Compliance of Asphalt Mixtures*, IDEA Program Final Report, NCHRP-133, June 2009.
4. Zofka, A., “Investigation of Asphalt Concrete Creep Behavior Using 3-Point Bending Test.” Ph.D. Thesis, University of Minnesota, Minneapolis, July 2007.
5. Zofka, A., Marasteanu, M., "Development of Double Edge Notched Tension (DENT) Test for Asphalt Binders", *Journal of Testing and Evaluation*, ASCE, Vol. 35, No. 3, 2007.
6. Li, X., “Investigation of the Fracture Resistance of Asphalt Mixtures at Low Temperature with a Semi Circular Bend (SCB) Test.” Ph.D. Thesis, University of Minnesota, Minneapolis, 2005.
7. Zhang W., Drescher A., Newcomb D. E., Viscoelastic analysis of diametral compression of asphalt concrete, *Journal of Engineering Mechanics*, Vol. 123, No. 6, 1997, pp. 596-603.